Mathematics

http://www.aimspress.com/journal/Math

AIMS Mathematics, 11(8): 24839–24876.
DOI: 10.3934/math.2026999
Received: 26 April 2026
Revised: 29 July 2026
Accepted: 06 August 2026
Published: 13 August 2026

Research article

The elliptic Dharwad index for structural characterizations of extremal graphs and QSPR applications

Suha Wazzan[1,*] **and Mohammed Alsharafi**[2,3]

[1] Department of Mathematics, Science Faculty, King Abdulaziz University, Jeddah 21589, Saudi Arabia

[2] Department of Mathematics, Faculty of Science, Sana'a University, Sana'a, Yemen

[3] Department of Mathematics, Faculty of Arts and Science, Yildiz Technical University, Esenler 34220, Istanbul, Turkey

* **Correspondence:** Email: swazzan@kau.edu.sa.

Abstract: Degree-based topological indices play an important role in chemical graph theory and network analysis, where structural heterogeneity is encoded through vertex degrees and aggregated over edges. In this paper, we introduce the *elliptic Dharwad index* (ED) of a simple graph $\mathcal{I}$,

$$ED(\mathcal{I}) = \sum_{uv \in E(\mathcal{I})} (d(u) + d(v)) \sqrt{d(u)^3 + d(v)^3},$$

and investigate its behavior under several fundamental graph operations and extremal constraints. We establish sharp lower and upper bounds for $ED(\mathcal{I} + \mathcal{J})$ and $ED(\mathcal{I} \odot \mathcal{J})$ in terms of the orders, sizes, and extremal degrees of the factors, together with complete equality characterizations. We also derive exact edge-decomposition formulas and degree-based bounds for the Cartesian product $\mathcal{I} \square \mathcal{J}$ and the tensor product $\mathcal{I} \otimes \mathcal{J}$, including an extension to k-fold Cartesian products. As further applications, we obtain closed forms for several standard graph families arising from joins and corona products, including paths, cycles, and complete graphs. On the extremal side, we prove that ED is strictly increasing under edge addition, determine sharp girth-based lower bounds for unicyclic graphs and connected graphs with a prescribed girth, and establish the best possible upper bound for connected graphs of order $\mathfrak{s}$ with exactly $\mathfrak{p}$ pendant vertices, showing that the unique extremal graph is $K_{\mathfrak{s},\mathfrak{p}}$. To complement the theoretical results, we examine ED in an exploratory univariate Quantitative Structure Property Relationship (QSPR) study on a dataset of 89 aromatic carboxylic acid, ester, and related benzenoid compounds, where the descriptor shows its clearest standalone signal for volumetric and size-related physicochemical properties. Overall, the results show that ED admits exact evaluation on important graph classes, satisfies sharp extremal principles, and has meaningful descriptive utility in chemical graph applications.

Keywords: elliptic Dharwad index; degree-based topological indices; graph operations; join; corona product; Cartesian product; tensor product; extremal graphs; girth; pendant vertices; QSPR
Mathematics Subject Classification: 05C09, 05C50, 05C92, 92E10

Abbreviations:

ED, elliptic Dharwad index; McVol, McGowan characteristic volume (mL mol^{-1}); V_c, critical volume (m^3 kmol^{-1}); $\Delta_f G^\circ$, standard Gibbs energy of formation (kJ mol^{-1}); $\Delta_{\text{fus}} H^\circ$, standard enthalpy of fusion (kJ mol^{-1}); $\log_{10}(W_S)$, logarithm of water solubility in mol L^{-1}; P_c, critical pressure (kPa); T_{boil}, normal boiling temperature (K); T_c, critical temperature (K); T_{fus}, normal melting/fusion temperature (K); $\log P_{\text{oct/wat}}$, octanol/water partition coefficient; $\Delta_f H^\circ_{\text{gas}}$, standard gas-phase enthalpy of formation (kJ mol^{-1}); $\Delta_{\text{vap}} H^\circ$, standard enthalpy of vaporization (kJ mol^{-1})

1. Introduction

Topological indices play a central role in chemical graph theory because they transform the structural features of a molecular graph into numerical descriptors that can be analyzed mathematically and used in structure–property studies. The early connection between graph invariants and molecular characteristics was already visible in the graph-theoretic treatment of molecular orbital energy by Gutman and Trinajstić [1]. A major milestone was the branching descriptor introduced by Randić [2], which demonstrated that graph-based quantities can capture chemically meaningful aspects of molecular structure.

Among the many classes of molecular descriptors, degree-based topological indices have attracted special attention because of their simple definition, broad applicability, and strong interaction with graph structure. Gutman [3] gave a systematic overview of degree-based indices and their mathematical significance. Nikolić et al. [4] and Gutman and Das [5] revisited the Zagreb indices and clarified their role within chemical graph theory. Xu et al. [6] later provided a detailed survey of Zagreb-type quantities, while Das [7] and Borovićanin et al. [8] developed sharp bounds and extremal results for these descriptors. Such studies show that degree-based invariants are not only chemically useful but also mathematically rich.

The continuing development of degree-based indices has led to many new descriptors designed to emphasize different aspects of local graph structure. Furtula and Gutman [9] revisited a neglected index and illustrated how seemingly simple degree-based expressions can reveal new structural information. Gagarin et al. [10] investigated generalized Zagreb indices, and Zhu et al. [11] studied further extensions and their extremal behavior. Hyper-Zagreb-type quantities have also been investigated in several graph-operation settings; for example, several authors [12–14] studied hyper-Zagreb indices and related coindices under different constructions.

A particularly active recent direction concerns Sombor-type descriptors. Gutman [15] introduced the geometric viewpoint behind Sombor indices, and Cruz et al. [16] studied the Sombor index of chemical graphs in detail. Das et al. [17] developed further mathematical properties of the Sombor index. Redžepović [18] examined its chemical applicability, while Wang et al. [19] investigated its relation to other degree-based descriptors. Extremal problems for Sombor-type indices have also received considerable attention: Ghanbari and Alikhani [20] evaluated these indices on specific graph classes, Chen et al. [21] studied trees with extremal Sombor values, Deng et al. [22] considered molecular trees with extremal Sombor behavior, and Li et al. [23] analyzed trees with a prescribed diameter.

In parallel with the Sombor literature, Dharwad-type descriptors have also appeared as new members of the degree-based family. Kulli [24] introduced Dharwad indices, and Kulli et al. [25] compared Dharwad, Sombor, Nirmala, and F-Sombor type quantities. More recently, elliptic-type variants have been proposed in order to strengthen the role of degree heterogeneity through nonlinear kernels. Gutman et al. [26] studied the elliptic Sombor index from both theoretical and applied viewpoints, and Espinal et al. [27] investigated the elliptic Sombor index of chemical graphs. These developments suggest that elliptic-type degree kernels can produce descriptors with both mathematical tractability and enhanced structural sensitivity.

Another important theme in the literature is the behavior of topological indices under graph operations. De et al. [28] considered the F-coindex under several graph operations. Akhter et al. [29] studied bounds for the general sum-connectivity index of composite graphs. Imran et al. [30] derived bounds for degree-based indices on Cartesian-product-related constructions. Oğuz Ünal [31] examined Sombor indices over tensor and Cartesian products. Alameri and Al-Sharafi [32] introduced topological-index formulas for new graph operations, and Alameri et al. [33] analyzed topological indices and coindices of disjunction and symmetric difference. These studies indicate that graph operations provide a natural setting in which one can obtain exact formulas, comparison principles, and extremal bounds for degree-based descriptors.

The chemical relevance of degree-based descriptors remains a major motivation for developing new indices. Hosamani et al. [34] performed Quantitative Structure Property Relationship (QSPR) analyses using degree-based topological indices, and Mondal et al. [35] showed that neighborhood-based degree descriptors can be informative in QSPR settings. Alameri and Alsharafi [36] discussed several types of topological indices and their applications, while Alsharafi et al. [37–39] explored the behavior of graph descriptors on nanotube- and nanotorus-related structures.

Recent studies have increasingly combined graph-theoretical descriptors with computational chemistry, external validation, and machine learning methods. Hakeem et al. [40] used degree-based descriptors in QSPR models for bioactive polyphenols, Alzahrani and Hanif [41] developed a machine learning QSPR framework based on graph invariants, and Song et al. [42] introduced cycle-configuration descriptors for machine learning-assisted molecular inference. In a large multi-task setting, Altairi et al. [43] further showed the value of testing newly designed graph descriptors together with complementary physicochemical features. These developments support the view that a new graph invariant should be examined both through rigorous structural analysis and through appropriately validated chemical applications.

Motivated by these developments, in this paper we introduce the *elliptic Dharwad index* (ED) of a simple graph $\mathcal{I}$ as follows:

$$ED(\mathcal{I}) = \sum_{uv \in E(\mathcal{I})} \left(d_{\mathcal{I}}(u) + d_{\mathcal{I}}(v)\right) \sqrt{d_{\mathcal{I}}(u)^3 + d_{\mathcal{I}}(v)^3}. \tag{1.1}$$

The construction combines two established ideas in a single edge kernel. Relative to the Dharwad index

$$D(\mathcal{I}) = \sum_{uv\in E(\mathcal{I})} \sqrt{d(u)^3 + d(v)^3},$$

it retains the cubic degree term and introduces the elliptic prefactor $d(u) + d(v)$; relative to the elliptic Sombor index

$$ESO(\mathcal{I}) = \sum_{uv\in E(\mathcal{I})} (d(u) + d(v)) \sqrt{d(u)^2 + d(v)^2},$$

it replaces the quadratic radial term by a cubic one [24,26]. For a fixed endpoint-degree sum, $d(u)^3+d(v)^3$ increases as the two degrees become more unequal, whereas on an edge of type (r, r), the contribution of ED grows as $2\sqrt{2}\, r^{5/2}$, compared with $\sqrt{2}\, r^{3/2}$ for the Dharwad index and $2\sqrt{2}\, r^2$ for the elliptic Sombor index. Thus, ED is designed to emphasize high-degree interactions while retaining sensitivity to the local degree imbalance.

The aim of the present work is twofold. On the mathematical side, we study the behavior of ED under several classical graph operations, including the join, corona product, Cartesian product, and tensor product. We derive exact formulas, sharp bounds, and regular-case equalities for these constructions, and we compute closed forms for several standard graph families. We also establish extremal results, including monotonicity under edge addition, girth-based lower bounds for unicyclic and connected graphs, and a sharp upper bound for graphs with a prescribed number of pendant vertices. On the applied side, we examine the descriptor in an exploratory univariate QSPR setting for a Cheméo-based dataset of aromatic carboxylic-acid, ester, and related benzenoid compounds. The results indicate that the elliptic Dharwad index is mathematically tractable, structurally expressive, and potentially useful as a compact screening descriptor in chemical graph applications.

2. Main results

In this section, we derive sharp lower and upper bounds for the elliptic Dharwad index under the join operation. We also record the corona product notation for later use. Recall that for a graph $\mathcal{I}$, the elliptic Dharwad index is defined in Eq (1.1).

2.1. Graph operations

Throughout this section, all graphs are assumed to be vertex-disjoint whenever a graph operation is applied.

Definition 2.1 (Join). *Let $\mathcal{I}$ and $\mathcal{J}$ be vertex-disjoint graphs. Their* join*, denoted $\mathcal{I} + \mathcal{J}$, is the graph with the vertex set $V(\mathcal{I} + \mathcal{J}) = V(\mathcal{I}) \cup V(\mathcal{J})$ and edge set*

$$E(\mathcal{I} + \mathcal{J}) = E(\mathcal{I}) \cup E(\mathcal{J}) \cup \{uv : \ u \in V(\mathcal{I}),\ v \in V(\mathcal{J})\}.$$

We reserve $\mathcal{I} \vee \mathcal{J}$ for the disjunction operation.

Definition 2.2 (Corona product). *Let $\mathcal{I}$ and $\mathcal{J}$ be graphs of orders $\mathfrak{s}_1$ and $\mathfrak{s}_2$, respectively. The* corona product *$\mathcal{I} \odot \mathcal{J}$ is obtained by taking one copy of $\mathcal{I}$ and, for each vertex $u \in V(\mathcal{I})$, attaching a private copy $\mathcal{J}^{(u)}$ of $\mathcal{J}$ and joining u to every vertex of $\mathcal{J}^{(u)}$.*

Remark 2.3. For $u \in V(\mathcal{I})$ and $v \in V(\mathcal{J})$, we have

$$d_{\mathcal{I}+\mathcal{J}}(u) = d_{\mathcal{I}}(u) + \mathfrak{s}_2, \qquad d_{\mathcal{I}+\mathcal{J}}(v) = d_{\mathcal{J}}(v) + \mathfrak{s}_1.$$

For the corona product, if $u \in V(\mathcal{I})$ and $v \in V(\mathcal{J}^{(u)})$, then

$$d_{\mathcal{I}\odot\mathcal{J}}(u) = d_{\mathcal{I}}(u) + \mathfrak{s}_2, \qquad d_{\mathcal{I}\odot\mathcal{J}}(v) = d_{\mathcal{J}}(v) + 1.$$

Moreover, $|E(\mathcal{I} \odot \mathcal{J})| = \mathrm{t}_1 + \mathfrak{s}_1\mathrm{t}_2 + \mathfrak{s}_1\mathfrak{s}_2$.

Theorem 2.4. *Let $\mathcal{I}$ and $\mathcal{J}$ be graphs of orders $\mathfrak{s}_1, \mathfrak{s}_2$ and sizes $\mathrm{t}_1, \mathrm{t}_2$, respectively. Then $\alpha_1 \leq ED(\mathcal{I} + \mathcal{J}) \leq \alpha_2$, where*

$$\begin{aligned}
\alpha_1 &= 2\sqrt{2}\,\mathrm{t}_1(\delta(\mathcal{I}) + \mathfrak{s}_2)^{5/2} + 2\sqrt{2}\,\mathrm{t}_2(\delta(\mathcal{J}) + \mathfrak{s}_1)^{5/2} \\
&\quad + \mathfrak{s}_1\mathfrak{s}_2(\delta(\mathcal{I}) + \mathfrak{s}_2 + \delta(\mathcal{J}) + \mathfrak{s}_1)\sqrt{(\delta(\mathcal{I}) + \mathfrak{s}_2)^3 + (\delta(\mathcal{J}) + \mathfrak{s}_1)^3}, \\
\alpha_2 &= 2\sqrt{2}\,\mathrm{t}_1(\Delta(\mathcal{I}) + \mathfrak{s}_2)^{5/2} + 2\sqrt{2}\,\mathrm{t}_2(\Delta(\mathcal{J}) + \mathfrak{s}_1)^{5/2} \\
&\quad + \mathfrak{s}_1\mathfrak{s}_2(\Delta(\mathcal{I}) + \mathfrak{s}_2 + \Delta(\mathcal{J}) + \mathfrak{s}_1)\sqrt{(\Delta(\mathcal{I}) + \mathfrak{s}_2)^3 + (\Delta(\mathcal{J}) + \mathfrak{s}_1)^3}.
\end{aligned}$$

Moreover, equality in either bound holds if and only if both $\mathcal{I}$ and $\mathcal{J}$ are regular.

Proof. Set

$$\Phi(x, y) = (x + y)\sqrt{x^3 + y^3}, \qquad x, y \geq 0.$$

Since Φ is increasing in each variable on $[0, \infty)$, the degree identities in Remark 2.3 imply

$$\begin{aligned}
ED(\mathcal{I} + \mathcal{J}) = &\sum_{uv\in E(\mathcal{I})} \Phi(d_{\mathcal{I}}(u) + \mathfrak{s}_2,\ d_{\mathcal{I}}(v) + \mathfrak{s}_2) \\
&+ \sum_{uv\in E(\mathcal{J})} \Phi(d_{\mathcal{J}}(u) + \mathfrak{s}_1,\ d_{\mathcal{J}}(v) + \mathfrak{s}_1) \\
&+ \sum_{u\in V(\mathcal{I})}\sum_{v\in V(\mathcal{J})} \Phi(d_{\mathcal{I}}(u) + \mathfrak{s}_2,\ d_{\mathcal{J}}(v) + \mathfrak{s}_1).
\end{aligned}$$

For every edge $uv \in E(\mathcal{I})$, $\delta(\mathcal{I}) + \mathfrak{s}_2 \leq d_{\mathcal{I}}(u) + \mathfrak{s}_2,\ d_{\mathcal{I}}(v) + \mathfrak{s}_2 \leq \Delta(\mathcal{I}) + \mathfrak{s}_2$. Hence

$$2\sqrt{2}\,(\delta(\mathcal{I}) + \mathfrak{s}_2)^{5/2} \leq \Phi(d_{\mathcal{I}}(u) + \mathfrak{s}_2,\ d_{\mathcal{I}}(v) + \mathfrak{s}_2) \leq 2\sqrt{2}\,(\Delta(\mathcal{I}) + \mathfrak{s}_2)^{5/2}.$$

After summing over the t_1 edges of $\mathcal{I}$, we obtain

$$2\sqrt{2}\,\mathrm{t}_1(\delta(\mathcal{I}) + \mathfrak{s}_2)^{5/2} \leq \sum_{uv\in E(\mathcal{I})} \Phi(\cdots) \leq 2\sqrt{2}\,\mathrm{t}_1(\Delta(\mathcal{I}) + \mathfrak{s}_2)^{5/2}.$$

Similarly we have

$$2\sqrt{2}\,\mathrm{t}_2(\delta(\mathcal{J}) + \mathfrak{s}_1)^{5/2} \leq \sum_{uv\in E(\mathcal{J})} \Phi(\cdots) \leq 2\sqrt{2}\,\mathrm{t}_2(\Delta(\mathcal{J}) + \mathfrak{s}_1)^{5/2}.$$

For each cross-edge uv with $u \in V(\mathcal{I})$ and $v \in V(\mathcal{J})$, monotonicity gives

$$\begin{aligned}
&(\delta(\mathcal{I}) + \mathfrak{s}_2 + \delta(\mathcal{J}) + \mathfrak{s}_1)\sqrt{(\delta(\mathcal{I}) + \mathfrak{s}_2)^3 + (\delta(\mathcal{J}) + \mathfrak{s}_1)^3} \\
\leq &\Phi(d_{\mathcal{I}}(u) + \mathfrak{s}_2,\ d_{\mathcal{J}}(v) + \mathfrak{s}_1) \\
\leq &(\Delta(\mathcal{I}) + \mathfrak{s}_2 + \Delta(\mathcal{J}) + \mathfrak{s}_1)\sqrt{(\Delta(\mathcal{I}) + \mathfrak{s}_2)^3 + (\Delta(\mathcal{J}) + \mathfrak{s}_1)^3}.
\end{aligned}$$

Since there are exactly $\mathfrak{s}_1\mathfrak{s}_2$ cross-edges, summing these bounds yields the desired inequality.

Finally, equality in either bound requires equality in every termwise estimate. That happens precisely when every vertex of $\mathcal{I}$ has the same degree and every vertex of $\mathcal{J}$ has the same degree; that is, when both $\mathcal{I}$ and $\mathcal{J}$ are regular. The converse is immediate. □

Corollary 2.5. *Let $\mathcal{I}$ and $\mathcal{J}$ be r_1- and r_2-regular graphs, respectively. We then have*

$$\begin{aligned}
ED(\mathcal{I} + \mathcal{J}) = &2\sqrt{2}\,\mathfrak{t}_1(r_1 + \mathfrak{s}_2)^{5/2} + 2\sqrt{2}\,\mathfrak{t}_2(r_2 + \mathfrak{s}_1)^{5/2} \\
&+ \mathfrak{s}_1\mathfrak{s}_2(r_1 + r_2 + \mathfrak{s}_1 + \mathfrak{s}_2)\sqrt{(r_1 + \mathfrak{s}_2)^3 + (r_2 + \mathfrak{s}_1)^3}.
\end{aligned}$$

Theorem 2.6. *Let $\mathcal{I}$ and $\mathcal{J}$ be graphs of orders $\mathfrak{s}_1, \mathfrak{s}_2$ and sizes $\mathfrak{t}_1, \mathfrak{t}_2$, respectively. Then*

$$\alpha_1 \leq ED(\mathcal{I} \odot \mathcal{J}) \leq \alpha_2,$$

where

$$\begin{aligned}
\alpha_1 = &2\sqrt{2}\,\mathfrak{t}_1(\delta(\mathcal{I}) + \mathfrak{s}_2)^{5/2} + 2\sqrt{2}\,\mathfrak{s}_1\mathfrak{t}_2(\delta(\mathcal{J}) + 1)^{5/2} \\
&+ \mathfrak{s}_1\mathfrak{s}_2(\delta(\mathcal{I}) + \mathfrak{s}_2 + \delta(\mathcal{J}) + 1)\sqrt{(\delta(\mathcal{I}) + \mathfrak{s}_2)^3 + (\delta(\mathcal{J}) + 1)^3}, \\
\alpha_2 = &2\sqrt{2}\,\mathfrak{t}_1(\Delta(\mathcal{I}) + \mathfrak{s}_2)^{5/2} + 2\sqrt{2}\,\mathfrak{s}_1\mathfrak{t}_2(\Delta(\mathcal{J}) + 1)^{5/2} \\
&+ \mathfrak{s}_1\mathfrak{s}_2(\Delta(\mathcal{I}) + \mathfrak{s}_2 + \Delta(\mathcal{J}) + 1)\sqrt{(\Delta(\mathcal{I}) + \mathfrak{s}_2)^3 + (\Delta(\mathcal{J}) + 1)^3}.
\end{aligned}$$

Moreover, equality in either bound holds if and only if both $\mathcal{I}$ and $\mathcal{J}$ are regular.

Proof. Let

$$\Phi(x, y) = (x + y)\sqrt{x^3 + y^3}, \qquad x, y \geq 0.$$

Since Φ is increasing in each variable on $[0, \infty)$, the degree relations from Remark 2.3 imply

$$\begin{aligned}
ED(\mathcal{I} \odot \mathcal{J}) = &\sum_{uv \in E(\mathcal{I})} \Phi(d_{\mathcal{I}}(u) + \mathfrak{s}_2,\ d_{\mathcal{I}}(v) + \mathfrak{s}_2) \\
&+ \mathfrak{s}_1 \sum_{xy \in E(\mathcal{J})} \Phi(d_{\mathcal{J}}(x) + 1,\ d_{\mathcal{J}}(y) + 1) \\
&+ \sum_{u \in V(\mathcal{I})} \sum_{v \in V(\mathcal{J}^{(u)})} \Phi(d_{\mathcal{I}}(u) + \mathfrak{s}_2,\ d_{\mathcal{J}}(v) + 1).
\end{aligned}$$

For every edge $uv \in E(\mathcal{I})$, we have

$$\delta(\mathcal{I}) + \mathfrak{s}_2 \leq d_{\mathcal{I}}(u) + \mathfrak{s}_2,\ d_{\mathcal{I}}(v) + \mathfrak{s}_2 \leq \Delta(\mathcal{I}) + \mathfrak{s}_2.$$

Hence,

$$2\sqrt{2}\,(\delta(\mathcal{I})+\mathfrak{s}_2)^{5/2} \le \Phi(d_{\mathcal{I}}(u)+\mathfrak{s}_2,\ d_{\mathcal{I}}(v)+\mathfrak{s}_2) \le 2\sqrt{2}\,(\Delta(\mathcal{I})+\mathfrak{s}_2)^{5/2}.$$

Summing over the t_1 edges of $\mathcal{I}$ gives

$$2\sqrt{2}\,\mathrm{t}_1(\delta(\mathcal{I})+\mathfrak{s}_2)^{5/2} \le \sum_{uv\in E(\mathcal{I})} \Phi(\cdots) \le 2\sqrt{2}\,\mathrm{t}_1(\Delta(\mathcal{I})+\mathfrak{s}_2)^{5/2}.$$

Similarly, for each edge $xy \in E(\mathcal{J})$, we have

$$2\sqrt{2}\,(\delta(\mathcal{J})+1)^{5/2} \le \Phi(d_{\mathcal{J}}(x)+1,\ d_{\mathcal{J}}(y)+1) \le 2\sqrt{2}\,(\Delta(\mathcal{J})+1)^{5/2},$$

and therefore

$$2\sqrt{2}\,\mathfrak{s}_1\mathrm{t}_2(\delta(\mathcal{J})+1)^{5/2} \le \mathfrak{s}_1 \sum_{xy\in E(\mathcal{J})} \Phi(\cdots) \le 2\sqrt{2}\,\mathfrak{s}_1\mathrm{t}_2(\Delta(\mathcal{J})+1)^{5/2}.$$

For each linking edge joining $u \in V(\mathcal{I})$ to $v \in V(\mathcal{J}^{(u)})$, monotonicity yields

$$\begin{aligned}
&(\delta(\mathcal{I})+\mathfrak{s}_2+\delta(\mathcal{J})+1)\sqrt{(\delta(\mathcal{I})+\mathfrak{s}_2)^3+(\delta(\mathcal{J})+1)^3}\\
\le&\Phi(d_{\mathcal{I}}(u)+\mathfrak{s}_2,\ d_{\mathcal{J}}(v)+1)\\
\le&(\Delta(\mathcal{I})+\mathfrak{s}_2+\Delta(\mathcal{J})+1)\sqrt{(\Delta(\mathcal{I})+\mathfrak{s}_2)^3+(\Delta(\mathcal{J})+1)^3}.
\end{aligned}$$

Since there are exactly $\mathfrak{s}_1\mathfrak{s}_2$ linking edges, summing these inequalities gives the required bounds.

Finally, equality in either bound holds precisely when equality occurs in every termwise estimate. This happens if and only if all vertices of $\mathcal{I}$ have the same degree and all vertices of $\mathcal{J}$ have the same degree, namely, if and only if both $\mathcal{I}$ and $\mathcal{J}$ are regular. □

Corollary 2.7. *Let $\mathcal{I}$ and $\mathcal{J}$ be r_1- and r_2-regular graphs, respectively. We then have*

$$\begin{aligned}
ED(\mathcal{I}\odot\mathcal{J}) = {}& 2\sqrt{2}\,\mathrm{t}_1(r_1+\mathfrak{s}_2)^{5/2} + 2\sqrt{2}\,\mathfrak{s}_1\mathrm{t}_2(r_2+1)^{5/2}\\
&+\mathfrak{s}_1\mathfrak{s}_2(r_1+\mathfrak{s}_2+r_2+1)\sqrt{(r_1+\mathfrak{s}_2)^3+(r_2+1)^3}.
\end{aligned}$$

2.2. *Closed forms for standard graph constructions*

We now derive explicit closed-form expressions for the elliptic Dharwad index for selected joins and corona products of standard graph families. We begin with the join of two paths.

Let $P_{\mathfrak{s}_1}$ and $P_{\mathfrak{s}_2}$ be paths of orders $\mathfrak{s}_1$ and $\mathfrak{s}_2$, respectively, where $\mathfrak{s}_1, \mathfrak{s}_2 \ge 2$. Then

$$\left|V(P_{\mathfrak{s}_1}+P_{\mathfrak{s}_2})\right| = \mathfrak{s}_1+\mathfrak{s}_2$$

and

$$\left|E(P_{\mathfrak{s}_1}+P_{\mathfrak{s}_2})\right| = (\mathfrak{s}_1-1)+(\mathfrak{s}_2-1)+\mathfrak{s}_1\mathfrak{s}_2 = \mathfrak{s}_1+\mathfrak{s}_2+\mathfrak{s}_1\mathfrak{s}_2-2.$$

Theorem 2.8. *For $\mathfrak{s}_1, \mathfrak{s}_2 \geq 2$, the elliptic Dharwad index of $P_{\mathfrak{s}_1} + P_{\mathfrak{s}_2}$ is given by*

$$ED(P_{\mathfrak{s}_1}+P_{\mathfrak{s}_2}) = \begin{cases} 108\sqrt{6}, \quad \mathfrak{s}_1 = \mathfrak{s}_2 = 2, \\ 2\sqrt{2}\,(\mathfrak{s}_2+1)^{5/2} + 14\sqrt{91} + 64(\mathfrak{s}_2-3)\sqrt{2} \\ \quad +4(\mathfrak{s}_2+4)\sqrt{(\mathfrak{s}_2+1)^3+27} + 2(\mathfrak{s}_2-2)(\mathfrak{s}_2+5)\sqrt{(\mathfrak{s}_2+1)^3+64}, \quad \mathfrak{s}_1 = 2,\ \mathfrak{s}_2 > 2, \\ 2\sqrt{2}\,(\mathfrak{s}_1+1)^{5/2} + 14\sqrt{91} + 64(\mathfrak{s}_1-3)\sqrt{2} \\ \quad +4(\mathfrak{s}_1+4)\sqrt{(\mathfrak{s}_1+1)^3+27} + 2(\mathfrak{s}_1-2)(\mathfrak{s}_1+5)\sqrt{(\mathfrak{s}_1+1)^3+64}, \quad \mathfrak{s}_2 = 2,\ \mathfrak{s}_1 > 2, \\ 2(2\mathfrak{s}_2+3)\sqrt{(\mathfrak{s}_2+1)^3+(\mathfrak{s}_2+2)^3} + (\mathfrak{s}_1-3)(2\mathfrak{s}_2+4)\sqrt{2(\mathfrak{s}_2+2)^3} \\ \quad +2(2\mathfrak{s}_1+3)\sqrt{(\mathfrak{s}_1+1)^3+(\mathfrak{s}_1+2)^3} + (\mathfrak{s}_2-3)(2\mathfrak{s}_1+4)\sqrt{2(\mathfrak{s}_1+2)^3} \\ \quad +4(\mathfrak{s}_1+\mathfrak{s}_2+2)\sqrt{(\mathfrak{s}_1+1)^3+(\mathfrak{s}_2+1)^3} \\ \quad +2(\mathfrak{s}_2-2)(\mathfrak{s}_1+\mathfrak{s}_2+3)\sqrt{(\mathfrak{s}_2+1)^3+(\mathfrak{s}_1+2)^3} \\ \quad +2(\mathfrak{s}_1-2)(\mathfrak{s}_1+\mathfrak{s}_2+3)\sqrt{(\mathfrak{s}_2+2)^3+(\mathfrak{s}_1+1)^3} \\ \quad +(\mathfrak{s}_1-2)(\mathfrak{s}_2-2)(\mathfrak{s}_1+\mathfrak{s}_2+4)\sqrt{(\mathfrak{s}_2+2)^3+(\mathfrak{s}_1+2)^3}, \quad \mathfrak{s}_1, \mathfrak{s}_2 > 2. \end{cases}$$

Proof. In the join $P_{\mathfrak{s}_1} + P_{\mathfrak{s}_2}$, the degrees satisfy

$$d_{P_{\mathfrak{s}_1}+P_{\mathfrak{s}_2}}(u) = d_{P_{\mathfrak{s}_1}}(u) + \mathfrak{s}_2 \quad (u \in V(P_{\mathfrak{s}_1})),$$

and

$$d_{P_{\mathfrak{s}_1}+P_{\mathfrak{s}_2}}(v) = d_{P_{\mathfrak{s}_2}}(v) + \mathfrak{s}_1 \quad (v \in V(P_{\mathfrak{s}_2})).$$

Since each path has two end vertices of degree 1 and all remaining vertices, when present are of degree 2, the vertices of $P_{\mathfrak{s}_1}$ in the join have degrees $\mathfrak{s}_2 + 1$ and $\mathfrak{s}_2 + 2$, while the vertices of $P_{\mathfrak{s}_2}$ in the join have degrees $\mathfrak{s}_1 + 1$ and $\mathfrak{s}_1 + 2$.

Accordingly, the edges of $P_{\mathfrak{s}_1} + P_{\mathfrak{s}_2}$ are split into the degree classes listed in Table 1.

Table 1. Edge partition of $P_{\mathfrak{s}_1} + P_{\mathfrak{s}_2}$ according to endpoint degrees.

Degree pair (a, b)	Number of edges	Condition
$(\mathfrak{s}_2+1, \mathfrak{s}_2+1)$	1	$\mathfrak{s}_1 = 2$
$(\mathfrak{s}_2+1, \mathfrak{s}_2+2)$	2	$\mathfrak{s}_1 > 2$
$(\mathfrak{s}_2+2, \mathfrak{s}_2+2)$	$\mathfrak{s}_1 - 3$	$\mathfrak{s}_1 > 2$
$(\mathfrak{s}_1+1, \mathfrak{s}_1+1)$	1	$\mathfrak{s}_2 = 2$
$(\mathfrak{s}_1+1, \mathfrak{s}_1+2)$	2	$\mathfrak{s}_2 > 2$
$(\mathfrak{s}_1+2, \mathfrak{s}_1+2)$	$\mathfrak{s}_2 - 3$	$\mathfrak{s}_2 > 2$
$(\mathfrak{s}_2+1, \mathfrak{s}_1+1)$	4	always
$(\mathfrak{s}_2+1, \mathfrak{s}_1+2)$	$2(\mathfrak{s}_2-2)$	$\mathfrak{s}_2 > 2$
$(\mathfrak{s}_2+2, \mathfrak{s}_1+1)$	$2(\mathfrak{s}_1-2)$	$\mathfrak{s}_1 > 2$
$(\mathfrak{s}_2+2, \mathfrak{s}_1+2)$	$(\mathfrak{s}_1-2)(\mathfrak{s}_2-2)$	$\mathfrak{s}_1, \mathfrak{s}_2 > 2$

For an edge with endpoint degrees (a, b), its contribution to the elliptic Dharwad index is

$$(a + b)\sqrt{a^3 + b^3}.$$

Summing these contributions over all edge classes yields the required expression. Evaluating the resulting sum in the four cases

$$(\mathfrak{s}_1, \mathfrak{s}_2) = (2, 2), \qquad \mathfrak{s}_1 = 2 < \mathfrak{s}_2, \qquad \mathfrak{s}_2 = 2 < \mathfrak{s}_1, \qquad \mathfrak{s}_1, \mathfrak{s}_2 > 2,$$

gives the stated formula. □

Theorem 2.9. *Let* $\mathfrak{s}_1, \mathfrak{s}_2 \geq 3$. *Then*

$$ED(C_{\mathfrak{s}_1} + C_{\mathfrak{s}_2}) = 2\sqrt{2}\,\mathfrak{s}_1(\mathfrak{s}_2 + 2)^{5/2} + 2\sqrt{2}\,\mathfrak{s}_2(\mathfrak{s}_1 + 2)^{5/2} + \mathfrak{s}_1\mathfrak{s}_2(\mathfrak{s}_1 + \mathfrak{s}_2 + 4)\sqrt{(\mathfrak{s}_1 + 2)^3 + (\mathfrak{s}_2 + 2)^3}.$$

Proof. In $C_{\mathfrak{s}_1} + C_{\mathfrak{s}_2}$, every vertex of $C_{\mathfrak{s}_1}$ has degree $\mathfrak{s}_2 + 2$, and every vertex of $C_{\mathfrak{s}_2}$ has degree $\mathfrak{s}_1 + 2$. Hence the edges are split into the following three classes:

$$(\mathfrak{s}_2 + 2, \mathfrak{s}_2 + 2), \qquad (\mathfrak{s}_1 + 2, \mathfrak{s}_1 + 2), \qquad (\mathfrak{s}_2 + 2, \mathfrak{s}_1 + 2),$$

with the multiplicities $\mathfrak{s}_1$, $\mathfrak{s}_2$, and $\mathfrak{s}_1\mathfrak{s}_2$, respectively.

For an edge whose endpoint degrees are (a, b), the contribution to ED is $(a + b)\sqrt{a^3 + b^3}$. Thus each edge of type (x, x) contributes

$$(2x)\sqrt{2x^3} = 2\sqrt{2}\,x^{5/2},$$

while each cross-edge contributes

$$(\mathfrak{s}_1 + \mathfrak{s}_2 + 4)\sqrt{(\mathfrak{s}_1 + 2)^3 + (\mathfrak{s}_2 + 2)^3}.$$

Summing over all three edge classes gives the required formula. □

Theorem 2.10. *Let* $\mathfrak{s}_1, \mathfrak{s}_2 \geq 1$. *Since*

$$K_{\mathfrak{s}_1} + K_{\mathfrak{s}_2} \cong K_{\mathfrak{s}_1+\mathfrak{s}_2},$$

we have

$$ED(K_{\mathfrak{s}_1} + K_{\mathfrak{s}_2}) = \sqrt{2}\,(\mathfrak{s}_1 + \mathfrak{s}_2)(\mathfrak{s}_1 + \mathfrak{s}_2 - 1)^{7/2}.$$

Proof. In $K_{\mathfrak{s}_1+\mathfrak{s}_2}$, every vertex has a degree

$$d = \mathfrak{s}_1 + \mathfrak{s}_2 - 1,$$

and the number of edges is

$$\left|E(K_{\mathfrak{s}_1+\mathfrak{s}_2})\right| = \frac{(\mathfrak{s}_1 + \mathfrak{s}_2)(\mathfrak{s}_1 + \mathfrak{s}_2 - 1)}{2}.$$

Each edge contributes

$$(2d)\sqrt{2d^3} = 2\sqrt{2}\,d^{5/2}.$$

Therefore, we have

$$ED(K_{\mathfrak{s}_1+\mathfrak{s}_2}) = \frac{(\mathfrak{s}_1 + \mathfrak{s}_2)(\mathfrak{s}_1 + \mathfrak{s}_2 - 1)}{2} \cdot 2\sqrt{2}\,d^{5/2} = \sqrt{2}\,(\mathfrak{s}_1 + \mathfrak{s}_2)d^{7/2},$$

which proves the claim. □

Theorem 2.11. *Let $\mathfrak{s}_1 \geq 3$ and $\mathfrak{s}_2 \geq 1$. We then have*

$$ED(C_{\mathfrak{s}_1} + K_{\mathfrak{s}_2}) = 2\sqrt{2}\,\mathfrak{s}_1(\mathfrak{s}_2+2)^{5/2} + \mathfrak{s}_1\mathfrak{s}_2(\mathfrak{s}_1+2\mathfrak{s}_2+1)\sqrt{(\mathfrak{s}_2+2)^3+(\mathfrak{s}_1+\mathfrak{s}_2-1)^3} + 2\sqrt{2}\binom{\mathfrak{s}_2}{2}(\mathfrak{s}_1+\mathfrak{s}_2-1)^{5/2}.$$

Proof. In $C_{\mathfrak{s}_1} + K_{\mathfrak{s}_2}$, each vertex of $C_{\mathfrak{s}_1}$ has degree $\mathfrak{s}_2 + 2$, while each vertex of $K_{\mathfrak{s}_2}$ has degree $\mathfrak{s}_1 + \mathfrak{s}_2 - 1$. Hence the edges are split into the following three classes:

$$(\mathfrak{s}_2+2, \mathfrak{s}_2+2), \qquad (\mathfrak{s}_2+2, \mathfrak{s}_1+\mathfrak{s}_2-1), \qquad (\mathfrak{s}_1+\mathfrak{s}_2-1, \mathfrak{s}_1+\mathfrak{s}_2-1),$$

with multiplicities $\mathfrak{s}_1$, $\mathfrak{s}_1\mathfrak{s}_2$, and $\binom{\mathfrak{s}_2}{2}$, respectively. Summing the corresponding contributions $(a+b)\sqrt{a^3+b^3}$ over these three classes yields the stated formula. □

Corollary 2.12. *Let $\mathcal{I} = C_{\mathfrak{s}_1}$ and $\mathcal{J} = K_{\mathfrak{s}_2}$ by Theorem 2.4. Then the value obtained in Theorem 2.11 agrees with the general regular-case expression from Theorem 2.4. In particular, since both $C_{\mathfrak{s}_1}$ and $K_{\mathfrak{s}_2}$ are regular, we have*

$$\alpha_1 = \alpha_2 = ED(C_{\mathfrak{s}_1} + K_{\mathfrak{s}_2}).$$

2.3. Closed forms for corona products of standard graphs

Theorem 2.13. *If we let $\mathfrak{s}_1, \mathfrak{s}_2 \geq 2$, then*

$$ED(P_{\mathfrak{s}_1} \odot P_{\mathfrak{s}_2}) = \begin{cases} 32 + 18\sqrt{6} + 20\sqrt{35}, & \mathfrak{s}_1 = \mathfrak{s}_2 = 2, \\ 2\sqrt{2}(\mathfrak{s}_2+1)^{5/2} + 20\sqrt{35} + 36(\mathfrak{s}_2-3)\sqrt{6} \\ \quad +4(\mathfrak{s}_2+3)\sqrt{(\mathfrak{s}_2+1)^3+8} + 2(\mathfrak{s}_2-2)(\mathfrak{s}_2+4)\sqrt{(\mathfrak{s}_2+1)^3+27}, & \mathfrak{s}_1 = 2,\ \mathfrak{s}_2 > 2, \\ 16\mathfrak{s}_1 + 14\sqrt{91} + 20\sqrt{35} + (136\mathfrak{s}_1 - 336)\sqrt{2}, & \mathfrak{s}_2 = 2,\ \mathfrak{s}_1 > 2, \\ 2(2\mathfrak{s}_2+3)\sqrt{(\mathfrak{s}_2+1)^3+(\mathfrak{s}_2+2)^3} + 2\sqrt{2}(\mathfrak{s}_1-3)(\mathfrak{s}_2+2)^{5/2} \\ \quad +10\mathfrak{s}_1\sqrt{35} + 18\mathfrak{s}_1(\mathfrak{s}_2-3)\sqrt{6} + 4(\mathfrak{s}_2+3)\sqrt{(\mathfrak{s}_2+1)^3+8} \\ \quad +2(\mathfrak{s}_2-2)(\mathfrak{s}_2+4)\sqrt{(\mathfrak{s}_2+1)^3+27} + 2(\mathfrak{s}_1-2)(\mathfrak{s}_2+4)\sqrt{(\mathfrak{s}_2+2)^3+8} \\ \quad +(\mathfrak{s}_1-2)(\mathfrak{s}_2-2)(\mathfrak{s}_2+5)\sqrt{(\mathfrak{s}_2+2)^3+27}, & \mathfrak{s}_1, \mathfrak{s}_2 > 2. \end{cases}$$

Proof. In $P_{\mathfrak{s}_1} \odot P_{\mathfrak{s}_2}$, each vertex of the base path $P_{\mathfrak{s}_1}$ has degree $\mathfrak{s}_2 + 1$ or $\mathfrak{s}_2 + 2$, while each vertex in a copy of $P_{\mathfrak{s}_2}$ has degree 2 or 3. Accordingly, the edge set splits into three groups: The edges of the base path, the edges inside the $\mathfrak{s}_1$ attached copies of $P_{\mathfrak{s}_2}$, and the linking edges between each base vertex and its private copy.

For an edge with endpoint degrees (a, b), the contribution to ED is

$$(a+b)\sqrt{a^3+b^3}.$$

Summing these contributions over all edge classes and simplifying in the four cases

$$(\mathfrak{s}_1, \mathfrak{s}_2) = (2,2), \qquad \mathfrak{s}_1 = 2 < \mathfrak{s}_2, \qquad \mathfrak{s}_2 = 2 < \mathfrak{s}_1, \qquad \mathfrak{s}_1, \mathfrak{s}_2 > 2,$$

gives the stated expression. □

Corollary 2.14. *If we let $\mathcal{I} = P_{\mathfrak{s}_1}$ and $\mathcal{J} = P_{\mathfrak{s}_2}$ in Theorem 2.6, then*

$$\alpha_1 \leq ED(P_{\mathfrak{s}_1} \odot P_{\mathfrak{s}_2}) \leq \alpha_2.$$

Theorem 2.15. *If we let $\mathfrak{s}_1, \mathfrak{s}_2 \geq 3$, then*

$$ED(C_{\mathfrak{s}_1} \odot C_{\mathfrak{s}_2}) = 18\mathfrak{s}_1\mathfrak{s}_2\sqrt{6} + \mathfrak{s}_1\mathfrak{s}_2(\mathfrak{s}_2+5)\sqrt{(\mathfrak{s}_2+2)^3+27} + 2\sqrt{2}\,\mathfrak{s}_1(\mathfrak{s}_2+2)^{5/2}.$$

Proof. In $C_{\mathfrak{s}_1} \odot C_{\mathfrak{s}_2}$, each vertex of the base cycle $C_{\mathfrak{s}_1}$ has degree $\mathfrak{s}_2 + 2$, while each vertex in an attached copy of $C_{\mathfrak{s}_2}$ has degree 3. Thus the edges are split into three classes as follows:

$$(3,3), \qquad (3, \mathfrak{s}_2+2), \qquad (\mathfrak{s}_2+2, \mathfrak{s}_2+2),$$

with the multiplicities $\mathfrak{s}_1\mathfrak{s}_2$, $\mathfrak{s}_1\mathfrak{s}_2$, and $\mathfrak{s}_1$, respectively. Summing the corresponding contributions $(a+b)\sqrt{a^3+b^3}$ yields the stated formula. □

Corollary 2.16. *Let $\mathcal{I} = C_{\mathfrak{s}_1}$ and $\mathcal{J} = C_{\mathfrak{s}_2}$ in Theorem 2.6. In this case the value in Theorem 2.15 agrees with the regular case equality in Theorem 2.6. In particular,*

$$\alpha_1 = \alpha_2 = ED(C_{\mathfrak{s}_1} \odot C_{\mathfrak{s}_2}).$$

Theorem 2.17. *If we let $\mathfrak{s}_1, \mathfrak{s}_2 \geq 1$, then,*

$$\begin{aligned} ED(K_{\mathfrak{s}_1} \odot K_{\mathfrak{s}_2}) = {} & 2\sqrt{2}\binom{\mathfrak{s}_1}{2}(\mathfrak{s}_1+\mathfrak{s}_2-1)^{5/2} \\ & + 2\sqrt{2}\,\mathfrak{s}_1\binom{\mathfrak{s}_2}{2}\mathfrak{s}_2^{5/2} + \mathfrak{s}_1\mathfrak{s}_2(\mathfrak{s}_1+2\mathfrak{s}_2-1)\sqrt{(\mathfrak{s}_1+\mathfrak{s}_2-1)^3+\mathfrak{s}_2^3}. \end{aligned}$$

Proof. In $K_{\mathfrak{s}_1} \odot K_{\mathfrak{s}_2}$, each vertex of $K_{\mathfrak{s}_1}$ has degree $(\mathfrak{s}_1-1)+\mathfrak{s}_2 = \mathfrak{s}_1+\mathfrak{s}_2-1$, while each vertex in a copy of $K_{\mathfrak{s}_2}$ has degree $(\mathfrak{s}_2-1)+1 = \mathfrak{s}_2$. Hence the edges are split into three classes: The edges of $K_{\mathfrak{s}_1}$, the edges inside the $\mathfrak{s}_1$ copies of $K_{\mathfrak{s}_2}$, and the $\mathfrak{s}_1\mathfrak{s}_2$ linking edges. Summing the contributions $(a+b)\sqrt{a^3+b^3}$ over these three classes gives the required expression. □

2.4. Elliptic Dharwad index of the Cartesian product

For $(u,v) \in V(\mathcal{I}\square\mathcal{J})$, the vertex degree satisfies

$$d_{\mathcal{I}\square\mathcal{J}}(u,v) = d_{\mathcal{I}}(u) + d_{\mathcal{J}}(v).$$

Theorem 2.18. *If we let $\mathcal{I}$ and $\mathcal{J}$ be graphs, then*

$$\begin{aligned} ED(\mathcal{I}\square\mathcal{J}) = {} & \sum_{v\in V(\mathcal{J})}\sum_{u_1u_2\in E(\mathcal{I})}\Big(d_{\mathcal{I}}(u_1)+d_{\mathcal{I}}(u_2)+2d_{\mathcal{J}}(v)\Big) \\ & \times \sqrt{\big(d_{\mathcal{I}}(u_1)+d_{\mathcal{J}}(v)\big)^3+\big(d_{\mathcal{I}}(u_2)+d_{\mathcal{J}}(v)\big)^3} \\ & + \sum_{u\in V(\mathcal{I})}\sum_{v_1v_2\in E(\mathcal{J})}\Big(2d_{\mathcal{I}}(u)+d_{\mathcal{J}}(v_1)+d_{\mathcal{J}}(v_2)\Big) \\ & \times \sqrt{\big(d_{\mathcal{I}}(u)+d_{\mathcal{J}}(v_1)\big)^3+\big(d_{\mathcal{I}}(u)+d_{\mathcal{J}}(v_2)\big)^3}. \end{aligned}$$

Proof. The edges of $\mathcal{I}\square\mathcal{J}$ are split into two disjoint classes as follows:

$$(u_1, v)(u_2, v) \quad \text{for } v \in V(\mathcal{J}),\ u_1u_2 \in E(\mathcal{I}),$$

and

$$(u, v_1)(u, v_2) \quad \text{for } u \in V(\mathcal{I}),\ v_1v_2 \in E(\mathcal{J}).$$

Using

$$d_{\mathcal{I}\square\mathcal{J}}(u, v) = d_{\mathcal{I}}(u) + d_{\mathcal{J}}(v),$$

together with the definition

$$ED(G) = \sum_{xy\in E(G)} (d_G(x) + d_G(y)) \sqrt{d_G(x)^3 + d_G(y)^3},$$

the contribution from the first class of edges gives the first double sum, while the contribution from the second class gives the second double sum. Summing both parts yields the result. □

Theorem 2.19. *Let $\mathcal{I}$ and $\mathcal{J}$ be graphs of orders $\mathfrak{s}_1, \mathfrak{s}_2$ and sizes $\mathfrak{t}_1, \mathfrak{t}_2$, respectively. Then*

$$\alpha_1 \leq ED(\mathcal{I}\square\mathcal{J}) \leq \alpha_2,$$

where

$$\alpha_1 = 2\sqrt{2}\,(\mathfrak{t}_1\mathfrak{s}_2 + \mathfrak{t}_2\mathfrak{s}_1)(\delta(\mathcal{I}) + \delta(\mathcal{J}))^{5/2},$$
$$\alpha_2 = 2\sqrt{2}\,(\mathfrak{t}_1\mathfrak{s}_2 + \mathfrak{t}_2\mathfrak{s}_1)(\Delta(\mathcal{I}) + \Delta(\mathcal{J}))^{5/2}.$$

Moreover, equality in either bound holds if and only if both $\mathcal{I}$ and $\mathcal{J}$ are regular.

Proof. Set

$$\Phi(x, y) = (x + y)\sqrt{x^3 + y^3}, \qquad x, y \geq 0.$$

Since Φ is increasing in each variable on $[0, \infty)$, and since every vertex $(u, v) \in V(\mathcal{I}\square\mathcal{J})$ satisfies

$$\delta(\mathcal{I}) + \delta(\mathcal{J}) \leq d_{\mathcal{I}\square\mathcal{J}}(u, v) \leq \Delta(\mathcal{I}) + \Delta(\mathcal{J}),$$

each edge of $\mathcal{I}\square\mathcal{J}$ contributes at least $2\sqrt{2}\,(\delta(\mathcal{I}) + \delta(\mathcal{J}))^{5/2}$ and at most $2\sqrt{2}\,(\Delta(\mathcal{I}) + \Delta(\mathcal{J}))^{5/2}$.

Now $|E(\mathcal{I}\square\mathcal{J})| = \mathfrak{t}_1\mathfrak{s}_2 + \mathfrak{t}_2\mathfrak{s}_1$. Multiplying the termwise lower and upper bounds by the number of edges gives $\alpha_1 \leq ED(\mathcal{I}\square\mathcal{J}) \leq \alpha_2$.

If both $\mathcal{I}$ and $\mathcal{J}$ are regular, then $\mathcal{I}\square\mathcal{J}$ is regular, and every edge contributes the same value, so equality holds in both bounds.

Conversely, equality in either bound forces every edge of $\mathcal{I}\square\mathcal{J}$ to attain the corresponding extremal value, and hence every vertex of $\mathcal{I}\square\mathcal{J}$ must have the same degree. Therefore, $\mathcal{I}\square\mathcal{J}$ is regular. Fixing $v \in V(\mathcal{J})$, the identity $d_{\mathcal{I}\square\mathcal{J}}(u, v) = d_{\mathcal{I}}(u) + d_{\mathcal{J}}(v)$ shows that $d_{\mathcal{I}}(u)$ is constant on $V(\mathcal{I})$, and so $\mathcal{I}$ is regular. Similarly, $\mathcal{J}$ is regular. □

Corollary 2.20. *If $\mathcal{I}$ and $\mathcal{J}$ are r_1- and r_2-regular graphs, respectively, then*

$$ED(\mathcal{I}\square\mathcal{J}) = 2\sqrt{2}\,(\mathfrak{t}_1\mathfrak{s}_2 + \mathfrak{t}_2\mathfrak{s}_1)(r_1 + r_2)^{5/2}.$$

Remark 2.21. Let $G_1, \ldots, G_k$ be graphs of orders $\mathfrak{s}_1, \ldots, \mathfrak{s}_k$ and sizes $\mathfrak{t}_1, \ldots, \mathfrak{t}_k$. For the Cartesian product $G_1 \square \cdots \square G_k$, we have

$$d_{G_1 \square \cdots \square G_k}(v_1, \ldots, v_k) = \sum_{i=1}^{k} d_{G_i}(v_i),$$

and

$$|E(G_1 \square \cdots \square G_k)| = \sum_{i=1}^{k} \mathfrak{t}_i \prod_{\substack{j=1 \\ j \neq i}}^{k} \mathfrak{s}_j.$$

Consequently, we have

$$2\sqrt{2}\,|E(G_1 \square \cdots \square G_k)| \Big(\sum_{i=1}^{k} \delta(G_i)\Big)^{5/2} \leq ED(G_1 \square \cdots \square G_k)$$

and

$$ED(G_1 \square \cdots \square G_k) \leq 2\sqrt{2}\,|E(G_1 \square \cdots \square G_k)| \Big(\sum_{i=1}^{k} \Delta(G_i)\Big)^{5/2}.$$

2.5. *Elliptic Dharwad index of the tensor product*

For $(a, b) \in V(\mathcal{I} \otimes \mathcal{J})$, the vertex degree satisfies $d_{\mathcal{I} \otimes \mathcal{J}}(a, b) = d_{\mathcal{I}}(a)\, d_{\mathcal{J}}(b)$. Moreover, $|E(\mathcal{I} \otimes \mathcal{J})| = 2\mathfrak{t}_1\mathfrak{t}_2$, since each pair of edges $u_1u_2 \in E(\mathcal{I})$ and $v_1v_2 \in E(\mathcal{J})$ generates the two edges $(u_1, v_1)(u_2, v_2)$ and $(u_1, v_2)(u_2, v_1)$ in $\mathcal{I} \otimes \mathcal{J}$.

Figure 1 illustrates the structure of the tensor product $P_5 \otimes C_5$.

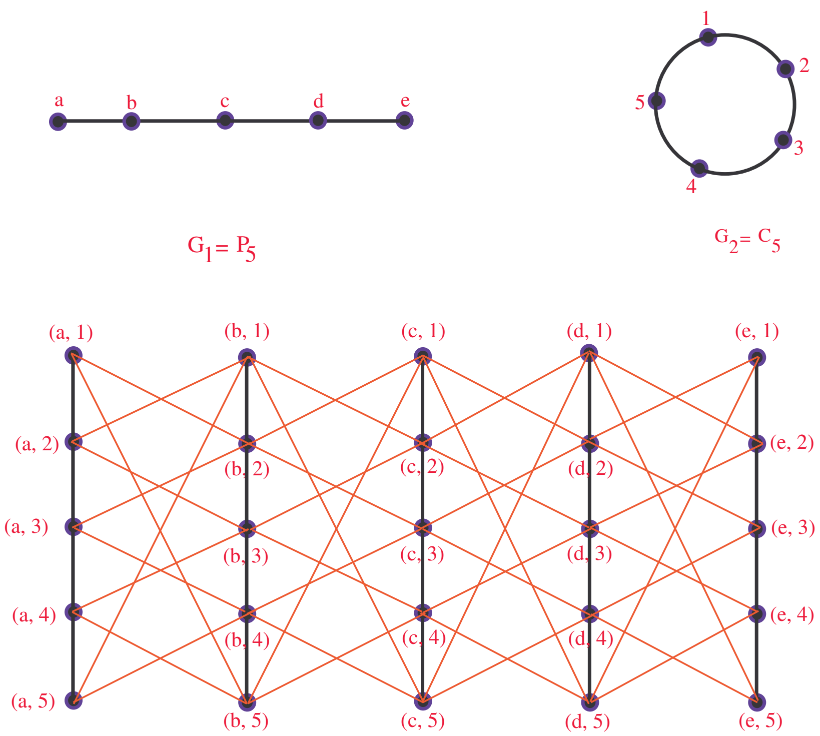

Figure 1. Tensor product $P_5 \otimes C_5$.

Theorem 2.22. *If we let $\mathcal{I}$ and $\mathcal{J}$ be graphs, then*

$$\begin{aligned} ED(\mathcal{I}\otimes\mathcal{J}) = &\sum_{u_1u_2\in E(\mathcal{I})}\sum_{v_1v_2\in E(\mathcal{J})}\Big(d_{\mathcal{I}}(u_1)d_{\mathcal{J}}(v_1)+d_{\mathcal{I}}(u_2)d_{\mathcal{J}}(v_2)\Big)\\ &\times\sqrt{\big(d_{\mathcal{I}}(u_1)d_{\mathcal{J}}(v_1)\big)^3+\big(d_{\mathcal{I}}(u_2)d_{\mathcal{J}}(v_2)\big)^3}\\ &+\sum_{u_1u_2\in E(\mathcal{I})}\sum_{v_1v_2\in E(\mathcal{J})}\Big(d_{\mathcal{I}}(u_1)d_{\mathcal{J}}(v_2)+d_{\mathcal{I}}(u_2)d_{\mathcal{J}}(v_1)\Big)\\ &\times\sqrt{\big(d_{\mathcal{I}}(u_1)d_{\mathcal{J}}(v_2)\big)^3+\big(d_{\mathcal{I}}(u_2)d_{\mathcal{J}}(v_1)\big)^3}. \end{aligned}$$

Proof. Fix $u_1u_2 \in E(\mathcal{I})$ and $v_1v_2 \in E(\mathcal{J})$. By definition of the tensor product, (u_1, v_1) is adjacent to (u_2, v_2), and (u_1, v_2) is adjacent to (u_2, v_1). Using $d_{\mathcal{I}\otimes\mathcal{J}}(a, b) = d_{\mathcal{I}}(a)d_{\mathcal{J}}(b)$ together with

$$ED(G) = \sum_{xy\in E(G)} (d_G(x) + d_G(y))\sqrt{d_G(x)^3 + d_G(y)^3},$$

and summing over all choices of u_1u_2 and v_1v_2, we obtain the required expression. □

Theorem 2.23. *Let $\mathcal{I}$ and $\mathcal{J}$ be graphs of sizes $\mathrm{t}_1, \mathrm{t}_2$, respectively. In this case*

$$\alpha_1 \le ED(\mathcal{I}\otimes\mathcal{J}) \le \alpha_2,$$

where

$$\begin{aligned} \alpha_1 &= 4\sqrt{2}\,\mathrm{t}_1\mathrm{t}_2(\delta(\mathcal{I})\delta(\mathcal{J}))^{5/2},\\ \alpha_2 &= 4\sqrt{2}\,\mathrm{t}_1\mathrm{t}_2(\Delta(\mathcal{I})\Delta(\mathcal{J}))^{5/2}. \end{aligned}$$

Moreover, equality in either bound holds if and only if both $\mathcal{I}$ and $\mathcal{J}$ are regular.

Proof. For any $(a, b) \in V(\mathcal{I}\otimes\mathcal{J})$, we have

$$\delta(\mathcal{I})\delta(\mathcal{J}) \le d_{\mathcal{I}\otimes\mathcal{J}}(a, b) \le \Delta(\mathcal{I})\Delta(\mathcal{J}).$$

Since

$$\Phi(x, y) = (x + y)\sqrt{x^3 + y^3}$$

is increasing in each variable on $[0, \infty)$, every edge of $\mathcal{I}\otimes\mathcal{J}$ contributes at least $2\sqrt{2}\,(\delta(\mathcal{I})\delta(\mathcal{J}))^{5/2}$ and at most $2\sqrt{2}\,(\Delta(\mathcal{I})\Delta(\mathcal{J}))^{5/2}$. Because

$$|E(\mathcal{I}\otimes\mathcal{J})| = 2\mathrm{t}_1\mathrm{t}_2,$$

multiplying these termwise bounds by the number of edges yields the stated inequalities.

If $\mathcal{I}$ and $\mathcal{J}$ are regular, then $\mathcal{I}\otimes\mathcal{J}$ is regular, so equality holds. Conversely, equality in either bound forces every vertex of $\mathcal{I}\otimes\mathcal{J}$ to have the same degree, which implies that both factors are regular. □

Corollary 2.24. *If $\mathcal{I}$ and $\mathcal{J}$ are r_1- and r_2-regular graphs, respectively, then*

$$ED(\mathcal{I}\otimes\mathcal{J}) = 4\sqrt{2}\,\mathrm{t}_1\mathrm{t}_2\,(r_1r_2)^{5/2}.$$

2.6. A unicyclic family and its elliptic Dharwad index

We next compute the elliptic Dharwad index of a unicyclic family parameterized by α and β, as illustrated in Figure 2.

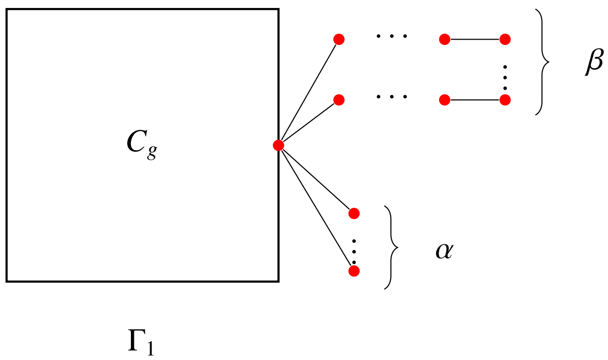

Figure 2. The unicyclic graph Γ_1 containing a cycle C_g.

Lemma 2.25. *Let Γ_1 be a unicyclic graph of order $\mathfrak{s}$ and girth g, where $g \le \mathfrak{s} - 2$. Assume that Γ_1 is obtained from the cycle C_g by attaching pendant edges and β pendant paths of length at least 2 to a fixed vertex α, where $\alpha, \beta \ge 0$. Set*

$$K := \alpha + \beta + 2.$$

Then

$$ED(\Gamma_1) = (\beta + 2)(K + 2)\sqrt{K^3 + 8} + 9\beta + \alpha(K + 1)\sqrt{K^3 + 1} + 16(\mathfrak{s} - \alpha - 2\beta - 2).$$

Proof. Let

$$\Phi(a, b) = (a + b)\sqrt{a^3 + b^3}.$$

The edges of Γ_1 fall into four classes according to the degrees of their endpoints.

First, the two cycle edges incident with the distinguished vertex, together with the first edges of the β long pendant paths, are all of type $(K, 2)$. Hence there are exactly $\beta + 2$ such edges.

Second, each pendant path of length at least 2 contributes exactly one terminal edge of type $(2, 1)$, so there are β edges of this type.

Third, each pendant edge contributes one edge of type $(K, 1)$, so there are α such edges.

Finally, all remaining edges are of type $(2, 2)$. The cycle contributes $g - 2$ such edges, and if the lengths of the β long pendant paths are $l_1, \ldots, l_\beta \ge 2$, then these paths contribute $(l_1 - 2) + \cdots + (l_\beta - 2)$ additional $(2, 2)$ edges. Since

$$\mathfrak{s} = g + \alpha + \sum_{i=1}^{\beta} l_i,$$

the total number of $(2, 2)$ edges is

$$(g - 2) + \sum_{i=1}^{\beta}(l_i - 2) = \mathfrak{s} - \alpha - 2\beta - 2.$$

For each edge type, the contribution to ED is:

$$\Phi(K, 2) = (K + 2)\sqrt{K^3 + 8}, \qquad \Phi(2, 1) = 9, \qquad \Phi(K, 1) = (K + 1)\sqrt{K^3 + 1}, \qquad \Phi(2, 2) = 16.$$

Multiplying by the corresponding multiplicities and summing gives the stated formula. □

For $3 \leq g \leq \mathfrak{s}$, let $C_{\mathfrak{s},g}$ denote the unicyclic graph of order $\mathfrak{s}$ and girth g obtained by attaching a pendant path of length $\mathfrak{s} - g$ to a fixed vertex of the cycle C_g. In the boundary case $g = \mathfrak{s}$, we set

$$C_{\mathfrak{s},g} \cong C_{\mathfrak{s}}.$$

Corollary 2.26. *Let Γ_1 be as in Lemma 2.25, with $g \leq \mathfrak{s} - 2$. In this case*

$$ED(\Gamma_1) \geq 16(\mathfrak{s} - 4) + 15\sqrt{35} + 9,$$

with equality if and only if $\Gamma_1 \cong C_{\mathfrak{s},g}$, or equivalently, if and only if $\alpha = 0$ and $\beta = 1$.

Proof. Since $g \leq \mathfrak{s} - 2$, we have $\mathfrak{s} - g \geq 2$. Therefore, at least one nontrivial pendant attachment is present, so $\alpha + \beta \geq 1$. Hence $K = \alpha + \beta + 2 \geq 3$.

If $\alpha + \beta = 1$, then the condition $g \leq \mathfrak{s} - 2$ forces the unique attachment to have a length of at least 2. Thus

$$(\alpha, \beta) = (0, 1), \qquad K = 3.$$

By Lemma 2.25, we have

$$ED(\Gamma_1) = 3 \cdot 5\sqrt{3^3 + 2^3} + 9 + 16(\mathfrak{s} - 4) = 16(\mathfrak{s} - 4) + 15\sqrt{35} + 9.$$

Now assume that $\alpha + \beta \geq 2$. Then $K \geq 4$, so the distinguished vertex has a larger degree than in the case $(\alpha, \beta) = (0, 1)$. Any additional attachment replaces at least one edge of type $(2, 2)$, whose contribution is 16, by one or more edges incident with a vertex of degree at least 3. Since $\Phi(a, b) = (a + b)\sqrt{a^3 + b^3}$ is strictly increasing in each variable for $a, b \geq 1$, every such replacement strictly increases the total value of ED. Therefore, we have

$$ED(\Gamma_1) > 16(\mathfrak{s} - 4) + 15\sqrt{35} + 9.$$

Hence the minimum is achieved uniquely for $(\alpha, \beta) = (0, 1)$; that is, precisely when $\Gamma_1 \cong C_{\mathfrak{s},g}$. □

2.7. *Girth-based minimum of ED for unicyclic graphs*

Theorem 2.27. *Let $\mathcal{I}$ be a unicyclic graph of order $\mathfrak{s} \geq 3$ and a girth g. Then*

$$ED(\mathcal{I}) \geq \begin{cases} 16\mathfrak{s}, & g = \mathfrak{s}, \\ 16(\mathfrak{s} - 3) + 10\sqrt{35} + 8\sqrt{7}, & g = \mathfrak{s} - 1, \\ 16(\mathfrak{s} - 4) + 15\sqrt{35} + 9, & g \leq \mathfrak{s} - 2. \end{cases}$$

Equality holds if and only if

$$\mathcal{I} \cong C_{\mathfrak{s}} \quad \text{when } g = \mathfrak{s},$$

$$\mathcal{I} \cong C_{\mathfrak{s},\mathfrak{s}-1} \quad \text{when } g = \mathfrak{s} - 1,$$

and

$$\mathcal{I} \cong C_{\mathfrak{s},g} \quad \text{when } g \leq \mathfrak{s} - 2.$$

Proof. If $g = \mathfrak{s}$, then $\mathcal{I} \cong C_{\mathfrak{s}}$, and every edge has the endpoint degrees $(2, 2)$. Hence

$$ED(\mathcal{I}) = \mathfrak{s} \cdot 16 = 16\mathfrak{s}.$$

If $g = \mathfrak{s} - 1$, then $\mathcal{I} \cong C_{\mathfrak{s},\mathfrak{s}-1}$. In this graph, there are $\mathfrak{s} - 3$ edges of type $(2, 2)$, two edges of type $(3, 2)$, and one edge of type $(3, 1)$. Therefore

$$ED(\mathcal{I}) = 16(\mathfrak{s} - 3) + 2 \cdot 5\sqrt{35} + 8\sqrt{7} = 16(\mathfrak{s} - 3) + 10\sqrt{35} + 8\sqrt{7}.$$

Now suppose $g \le \mathfrak{s} - 2$. Let q be the number of vertices of degree at least 3.

If $q = 1$, then $\mathcal{I} \cong \Gamma_1$, and Corollary 2.26 gives

$$ED(\mathcal{I}) \ge 16(\mathfrak{s} - 4) + 15\sqrt{35} + 9,$$

with equality if and only if $\mathcal{I} \cong C_{\mathfrak{s},g}$.

If $q \ge 2$, then one needs the additional structural fact that such a graph contains enough edges incident with branching vertices to force a strictly larger total than the case $q = 1$. In particular, every extra branching attachment increases the total contribution beyond that of the extremal graph $C_{\mathfrak{s},g}$, because the function

$$\Phi(a, b) = (a + b)\sqrt{a^3 + b^3}$$

is strictly increasing in each variable for $a, b \ge 1$. Hence

$$ED(\mathcal{I}) > 16(\mathfrak{s} - 4) + 15\sqrt{35} + 9.$$

Therefore, the minimum in the case $g \le \mathfrak{s} - 2$ is achieved uniquely by $C_{\mathfrak{s},g}$. □

Lemma 2.28. *Let $\mathcal{I}$ be a graph, and let $uv \notin E(\mathcal{I})$. If $\mathcal{I} + uv$ denotes the graph obtained from $\mathcal{I}$ by adding the edge uv, then*

$$ED(\mathcal{I}) < ED(\mathcal{I} + uv).$$

Proof. Adding the edge uv creates a new positive contribution

$$(d_{\mathcal{I}}(u) + 1 + d_{\mathcal{I}}(v) + 1)\sqrt{(d_{\mathcal{I}}(u) + 1)^3 + (d_{\mathcal{I}}(v) + 1)^3},$$

and every existing edge incident to u or v also contributes more, since

$$\Phi(a, b) = (a + b)\sqrt{a^3 + b^3}$$

is strictly increasing in each variable for $a, b \ge 1$. Hence

$$ED(\mathcal{I} + uv) > ED(\mathcal{I}).$$

□

Theorem 2.29. *Let $\mathcal{I}$ be a connected graph of order $\mathfrak{s} \ge 3$ and a girth g. Then*

$$ED(\mathcal{I}) \ge \begin{cases} 16\mathfrak{s}, & g = \mathfrak{s}, \\ 16(\mathfrak{s} - 3) + 10\sqrt{35} + 8\sqrt{7}, & g = \mathfrak{s} - 1, \\ 16(\mathfrak{s} - 4) + 15\sqrt{35} + 9, & g \le \mathfrak{s} - 2. \end{cases}$$

Equality holds if and only if

$$\mathcal{I} \cong C_{\mathfrak{s}} \quad \text{when } g = \mathfrak{s},$$

$$\mathcal{I} \cong C_{\mathfrak{s},\mathfrak{s}-1} \quad \text{when } g = \mathfrak{s} - 1,$$

and

$$\mathcal{I} \cong C_{\mathfrak{s},g} \quad \text{when } g \leq \mathfrak{s} - 2.$$

Proof. Choose a cycle of length g in $\mathcal{I}$. Since $\mathcal{I}$ is connected, there is a spanning tree T of $\mathcal{I}$ containing all vertices of $\mathcal{I}$ and all but one edge of that chosen cycle. Let e be the missing edge of the chosen cycle, and set $\mathcal{J} := T + e$. Then $\mathcal{J}$ is a spanning connected subgraph of $\mathcal{I}$ with

$$|V(\mathcal{J})| = \mathfrak{s}, \qquad |E(\mathcal{J})| = \mathfrak{s},$$

so $\mathcal{J}$ is unicyclic. Moreover, $\mathcal{J}$ contains the chosen cycle of length g, and since a unicyclic graph has exactly one cycle, its girth is also g.

Now $\mathcal{I}$ is obtained from $\mathcal{J}$ by adding edges. By repeated application of Lemma 2.28, we have

$$ED(\mathcal{I}) \geq ED(\mathcal{J}),$$

with equality if and only if $\mathcal{I} \cong \mathcal{J}$.

Applying Theorem 2.27 to $\mathcal{J}$ yields the required lower bound and the equality characterization. □

Corollary 2.30. *Among all unicyclic graphs of order* $\mathfrak{s} \geq 3$*, the unique graph minimizing ED is the cycle* $C_{\mathfrak{s}}$*, and the minimum value is* $16\mathfrak{s}$*.*

Proof. This follows immediately from Theorem 2.27 by comparing the three girth cases. □

2.8. Graphs with a fixed number of pendant vertices: extremal setup

We next study the maximum value of the elliptic Dharwad index among connected graphs of fixed order and with a fixed number of pendant vertices.

Lemma 2.31 ([44,45])**.** *If* f *is convex and* $a, b \geq 0$*, then*

$$f(y) - f(y-a) \geq f(y-b) - f(y-b-a),$$

with equality if and only if $ab = 0$*.*

Let $\mathfrak{s}$ and $\mathfrak{p}$ be integers with $\mathfrak{s} > \mathfrak{p} \geq 0$. Define $K_{\mathfrak{s},\mathfrak{p}}$ to be the graph of order $\mathfrak{s}$ obtained by attaching $\mathfrak{p}$ pendant vertices to a single vertex of the complete graph $K_{\mathfrak{s}-\mathfrak{p}}$. In particular,

$$K_{\mathfrak{s},0} \cong K_{\mathfrak{s}}, \qquad K_{\mathfrak{s},\mathfrak{s}-1} \cong S_{\mathfrak{s}},$$

where $S_{\mathfrak{s}}$ denotes the star graph of order $\mathfrak{s}$.

Now let $0 \leq \mathfrak{p} \leq \mathfrak{s} - 2$, and let $a_1, a_2, \ldots, a_{\mathfrak{s}-\mathfrak{p}}$ be non-negative integers satisfying

$$\sum_{i=1}^{\mathfrak{s}-\mathfrak{p}} a_i = \mathfrak{p}.$$

We write $S(a_1, a_2, \ldots, a_{\mathfrak{s}-\mathfrak{p}})$ for the graph obtained from the complete graph $K_{\mathfrak{s}-\mathfrak{p}}$ by attaching a_i pendant vertices to its ith vertex, for each $i = 1, 2, \ldots, \mathfrak{s} - \mathfrak{p}$.

The next theorem gives an upper bound for the elliptic Dharwad index among connected graphs of order $\mathfrak{s}$ with exactly $\mathfrak{p}$ pendant vertices, together with the extremal graph.

Theorem 2.32. *Let $\mathcal{I}$ be a connected graph of order $\mathfrak{s}$ with exactly $\mathfrak{p}$ pendant vertices. Then*

$$
\begin{aligned}
ED(\mathcal{I}) \leq &\binom{\mathfrak{s}-\mathfrak{p}-1}{2} 2\sqrt{2}\,(\mathfrak{s}-\mathfrak{p}-1)^{5/2} \\
&+ (\mathfrak{s}-\mathfrak{p}-1)(2\mathfrak{s}-\mathfrak{p}-2)\sqrt{(\mathfrak{s}-1)^3+(\mathfrak{s}-\mathfrak{p}-1)^3} \\
&+ \mathfrak{p}\,\mathfrak{s}\sqrt{(\mathfrak{s}-1)^3+1},
\end{aligned}
\tag{2.1}
$$

with equality if and only if $\mathcal{I} \cong K_{\mathfrak{s},\mathfrak{p}}$.

Proof. If $\mathfrak{p} = \mathfrak{s}-1$, then $\mathcal{I} \cong S_{\mathfrak{s}} \cong K_{\mathfrak{s},\mathfrak{s}-1}$, so the statement is immediate. Thus we may assume $0 \leq \mathfrak{p} \leq \mathfrak{s}-2$.

Let U be the set of non-pendant vertices of $\mathcal{I}$. Since $\mathcal{I}$ is connected and has exactly $\mathfrak{p}$ pendant vertices, every pendant vertex is adjacent to a vertex of U, and $|U| = \mathfrak{s}-\mathfrak{p}$. By repeatedly adding all missing edges among vertices of U, Lemma 2.28 yields

$$
ED(\mathcal{I}) \leq ED(S(a_1, a_2, \ldots, a_{\mathfrak{s}-\mathfrak{p}})),
\tag{2.2}
$$

for some non-negative integers $a_1, \ldots, a_{\mathfrak{s}-\mathfrak{p}}$ satisfying

$$
\sum_{i=1}^{\mathfrak{s}-\mathfrak{p}} a_i = \mathfrak{p}.
$$

Moreover, the equality in (2.2) holds if and only if $\mathcal{I} \cong S(a_1, a_2, \ldots, a_{\mathfrak{s}-\mathfrak{p}})$.

Without loss of generality, relabel the vertices so that

$$
a_1 = \max\{a_j : \ 1 \leq j \leq \mathfrak{s}-\mathfrak{p}\}.
$$

If $a_1 = \mathfrak{p}$ and $a_2 = \cdots = a_{\mathfrak{s}-\mathfrak{p}} = 0$, then

$$
S(a_1, a_2, \ldots, a_{\mathfrak{s}-\mathfrak{p}}) \cong K_{\mathfrak{s},\mathfrak{p}}.
$$

We now compute the elliptic Dharwad index of $K_{\mathfrak{s},\mathfrak{p}}$. Its edges fall into the following three classes according to the endpoint degrees:

$$
(\mathfrak{s}-\mathfrak{p}-1, \mathfrak{s}-\mathfrak{p}-1) \quad \text{with multiplicity} \binom{\mathfrak{s}-\mathfrak{p}-1}{2},
$$

$$
(\mathfrak{s}-1, \mathfrak{s}-\mathfrak{p}-1) \quad \text{with multiplicity } \mathfrak{s}-\mathfrak{p}-1,
$$

and

$$
(\mathfrak{s}-1, 1) \quad \text{with multiplicity } \mathfrak{p}.
$$

Hence

$$
\begin{aligned}
ED(K_{\mathfrak{s},\mathfrak{p}}) = &\binom{\mathfrak{s}-\mathfrak{p}-1}{2}(2(\mathfrak{s}-\mathfrak{p}-1))\sqrt{2(\mathfrak{s}-\mathfrak{p}-1)^3} \\
&+ (\mathfrak{s}-\mathfrak{p}-1)(2\mathfrak{s}-\mathfrak{p}-2)\sqrt{(\mathfrak{s}-1)^3+(\mathfrak{s}-\mathfrak{p}-1)^3} + \mathfrak{p}\,\mathfrak{s}\sqrt{(\mathfrak{s}-1)^3+1}
\end{aligned}
$$

$$= \binom{\mathfrak{s}-\mathfrak{p}-1}{2} 2\sqrt{2}\,(\mathfrak{s}-\mathfrak{p}-1)^{5/2}$$
$$+ (\mathfrak{s}-\mathfrak{p}-1)(2\mathfrak{s}-\mathfrak{p}-2)\sqrt{(\mathfrak{s}-1)^3+(\mathfrak{s}-\mathfrak{p}-1)^3} + \mathfrak{p}\,\mathfrak{s}\sqrt{(\mathfrak{s}-1)^3+1}.$$

Combining this identity with (2.2), we obtain the bound (2.1) whenever $S(a_1, a_2, \ldots, a_{\mathfrak{s}-\mathfrak{p}}) \cong K_{\mathfrak{s},\mathfrak{p}}$.

It remains to show that if $a_1 < \mathfrak{p}$, then the value of $ED(S(a_1, \ldots, a_{\mathfrak{s}-\mathfrak{p}}))$ can be strictly increased by transferring one pendant edge from some vertex with $a_i \geq 1$ to the vertex carrying a_1 pendant edges. Repeating this transfer step eventually yields $K_{\mathfrak{s},\mathfrak{p}}$.

Assume that $a_1 < \mathfrak{p}$. Choose an index $i \geq 2$ such that $a_i \geq 1$, and let $\Gamma \cong S(a_1, a_2, \ldots, a_{\mathfrak{s}-\mathfrak{p}})$ and

$$\Gamma' \cong S(a_1+1, a_2, \ldots, a_{i-1}, a_i - 1, a_{i+1}, \ldots, a_{\mathfrak{s}-\mathfrak{p}}).$$

Set

$$t := \mathfrak{s}-\mathfrak{p}-1, \qquad A := t + a_1, \qquad B := t + a_i, \qquad C_j := t + a_j \quad (j \neq 1, i).$$

Thus, in Γ, the relevant clique-vertex degrees are A, B, C_j, whereas in Γ', they become $A+1, B-1, C_j$.

A direct comparison of all edge contributions that change gives

$$\begin{aligned} ED(\Gamma') - ED(\Gamma) = &\Big[(A+B)\sqrt{(A+1)^3+(B-1)^3} - (A+B)\sqrt{A^3+B^3}\Big] \\ &+ \Big[h(a_1+1) - h(a_1)\Big] - \Big[h(a_i) - h(a_i-1)\Big] \\ &+ \sum_{\substack{j=2 \\ j\neq i}}^{\mathfrak{s}-\mathfrak{p}} \Big[g_{C_j}(a_1+1) - g_{C_j}(a_1)\Big] \\ &- \sum_{\substack{j=2 \\ j\neq i}}^{\mathfrak{s}-\mathfrak{p}} \Big[g_{C_j}(a_i) - g_{C_j}(a_i-1)\Big], \end{aligned} \tag{2.3}$$

where

$$h(x) := x(t+x+1)\sqrt{(t+x)^3+1}, \qquad x \geq 0.$$

For each fixed $C > 0$,

$$g_C(x) := (t+x+C)\sqrt{(t+x)^3+C^3}, \qquad x \geq 0.$$

We now show that every grouped contribution in (2.3) is positive.

Claim 2.33. $(A+1)^3 + (B-1)^3 > A^3 + B^3$. *Consequently, we have*

$$(A+B)\sqrt{(A+1)^3+(B-1)^3} > (A+B)\sqrt{A^3+B^3}.$$

Proof. Since $a_1 \geq a_i$, we have $A \geq B$. Therefore

$$\begin{aligned} (A+1)^3 + (B-1)^3 - (A^3+B^3) &= 3A^2 + 3A + 1 - (3B^2 - 3B + 1) \\ &= 3(A^2 - B^2) + 3(A+B) > 0. \end{aligned}$$

Because $A + B > 0$, the second inequality follows immediately. □

Claim 2.34. *$h(a_1+1)-h(a_1) > h(a_i)-h(a_i-1)$. Equivalently, we have*

$$\Big[h(a_1+1)-h(a_1)\Big]-\Big[h(a_i)-h(a_i-1)\Big] > 0.$$

Proof. A direct differentiation shows that h is strictly convex on $[0,\infty)$. Apply Lemma 2.31 to h with

$$y = a_1+1, \qquad a = 1, \qquad b = a_1 - a_i + 1 > 0.$$

Then $h(a_1+1)-h(a_1) \geq h(a_i)-h(a_i-1)$. Since $a = 1$ and $b > 0$, equality is impossible by Lemma 2.31. Hence $h(a_1+1)-h(a_1) > h(a_i)-h(a_i-1)$. □

Claim 2.35. *For every fixed $C > 0$, $g_C(a_1+1)-g_C(a_1) > g_C(a_i)-g_C(a_i-1)$. Consequently,*

$$\sum_{\substack{j=2\\ j\neq i}}^{\mathfrak{s}-\mathfrak{p}}\Big[g_{C_j}(a_1+1)-g_{C_j}(a_1)\Big]-\sum_{\substack{j=2\\ j\neq i}}^{\mathfrak{s}-\mathfrak{p}}\Big[g_{C_j}(a_i)-g_{C_j}(a_i-1)\Big] > 0.$$

Proof. For each fixed $C > 0$, a direct differentiation shows that g_C is strictly convex on $[0,\infty)$. Applying Lemma 2.31 to g_C with $y = a_1+1,\ a = 1,\ b = a_1 - a_i + 1 > 0$, we obtain

$$g_C(a_1+1)-g_C(a_1) \geq g_C(a_i)-g_C(a_i-1).$$

Again, equality is impossible because $a = 1$ and $b > 0$. Thus

$$g_C(a_1+1)-g_C(a_1) > g_C(a_i)-g_C(a_i-1).$$

Taking $C = C_j$ and summing over all $j \neq 1, i$ proves the claim. □

Using Claims 2.33–2.35 in (2.3), we conclude that $ED(\Gamma') - ED(\Gamma) > 0$. Hence $ED(\Gamma') > ED(\Gamma)$.

Therefore, whenever $a_1 < \mathfrak{p}$, transferring one pendant edge from a vertex with $a_i \geq 1$ to the vertex carrying a_1 pendant edges strictly increases the elliptic Dharwad index. Repeating this transfer finitely many times yields

$$ED(S(a_1, a_2, \ldots, a_{\mathfrak{s}-\mathfrak{p}})) < ED(S(\mathfrak{p}, 0, \ldots, 0)) = ED(K_{\mathfrak{s},\mathfrak{p}}),$$

unless $a_1 = \mathfrak{p}$ already.

Combining this with (2.2), we obtain $ED(\mathcal{I}) \leq ED(K_{\mathfrak{s},\mathfrak{p}})$, and equality holds if and only if $\mathcal{I} \cong K_{\mathfrak{s},\mathfrak{p}}$. □

3. Quantitative structure–property relationship models via the elliptic Dharwad index

3.1. Dataset and physicochemical properties

Dataset composition and identifiers. The QSPR analysis was carried out on a Chemeo-derived dataset of aromatic carboxylic acids, esters, and closely related benzenoid derivatives. The original spreadsheet contained 90 entries. After checking structural identity through International Chemical Identifier Key (InChIKey) matching, one duplicated structure was removed, leaving a final dataset of $n = 89$ unique compounds. For each compound, the spreadsheet records the compound name, molecular formula, canonical Simplified Molecular Input Line Entry System (SMILES), InChI, InChIKey, and the basic graph-size quantities n_{atoms} and n_{bonds}. The curated compound-level dataset used in the present analysis is provided in Supplementary 1.

Physicochemical endpoints. The final dataset contains 12 continuous physicochemical responses: McGowan characteristic volume (McVol), critical volume (V_c), the standard Gibbs energy of formation ($\Delta_f G^\circ$), the standard enthalpy of fusion ($\Delta_{\text{fus}} H^\circ$), water solubility ($\log_{10}(W_S)$), critical pressure ($P_c$), normal boiling temperature (T_{boil}), critical temperature (T_c), fusion temperature (T_{fus}), octanol/water partition coefficient ($\log P_{\text{oct/wat}}$), standard gas-phase enthalpy of formation ($\Delta_f H^\circ_{\text{gas}}$), and standard enthalpy of vaporization ($\Delta_{\text{vap}} H^\circ$). The resulting modeling matrix is complete, with no missing values for the predictor or for any of the 12 responses.

Predictor descriptor. For each molecular graph $\mathcal{I}$, the sole predictor used in this section is the elliptic Dharwad index

$$ED(\mathcal{I}) = \sum_{uv \in E(\mathcal{I})} (d(u) + d(v)) \sqrt{d(u)^3 + d(v)^3},$$

where $d(u)$ and $d(v)$ denote the degrees of the end-vertices of the edge uv. This scalar degree-based descriptor aggregates weighted edge contributions across the molecular graph. For the present dataset, the computed ED values range from 258.84 to 1142.85, with a mean of 484.56 and a standard deviation of 165.05, indicating a broad spread in structural complexity.

Worked example: Aspirin. To make the descriptor construction explicit, consider aspirin (see Figure 3), whose canonical SMILES is `CC(=O)Oc1ccccc1C(=O)O`.

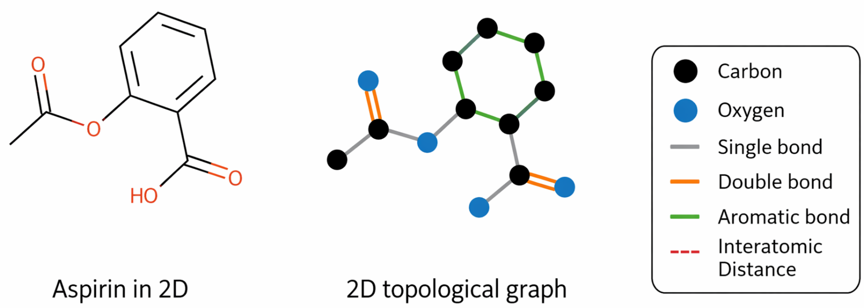

Figure 3. Aspirin structure and its hydrogen-suppressed molecular graph.

Its hydrogen-suppressed molecular graph has the edge-degree pattern $(1,3)^4,\ (2,3)^4,\ (2,2)^3,\ (3,3)^2$. Therefore, we have

$$\begin{aligned} ED &= 4(1+3)\sqrt{1^3+3^3} + 4(2+3)\sqrt{2^3+3^3} + 3(2+2)\sqrt{2^3+2^3} + 2(3+3)\sqrt{3^3+3^3} \\ &= 4(4)\sqrt{28} + 4(5)\sqrt{35} + 3(4)\sqrt{16} + 2(6)\sqrt{54} \approx 339.17. \end{aligned}$$

This agrees with the value reported for aspirin in Table 2.

The full compound-level values of ED and the 12 physicochemical endpoints are listed in Tables 2 and 3. A complete panel of the molecular structures of all studied compounds is available from: `https://www.chemeo.com/similar?smiles=CC%28%3dO%29Oc1ccccc1C%28%3dO%29O`.

Table 2. Physicochemical properties and the elliptic Dharwad index for the studied compounds (n = 89), Part I.

Compound	Formula	ED	McVol	V_c	$\Delta_f G^\circ$	$\Delta_{\text{fus}} H^\circ$	$\log_{10}(W_S)$	P_c	T_{boil}	T_c	T_{fus}	$\log P_{\text{oct/wat}}$	$\Delta_f H^\circ_{\text{gas}}$	$\Delta_{\text{vap}} H^\circ$
C_1	$C_9H_8O_4$	339.17	128.79	0.480	-371.98	33.85	-1.70	4082.92	659.32	868.49	322.40	1.310	-513.64	71.15
C_2	$C_{10}H_{10}O_4$	356.58	142.88	0.536	-363.56	23.78	-2.26	3624.61	682.20	888.42	424.31	1.700	-534.28	73.37
C_3	$C_9H_{10}O_3$	292.25	127.22	0.474	-243.06	19.59	-2.07	3773.04	605.45	807.67	363.11	1.783	-401.06	64.40
C_4	$C_{10}H_{10}O_4$	356.58	142.88	0.535	-331.74	20.88	-2.03	3191.93	612.44	831.50	385.72	1.398	-514.27	59.10
C_5	$C_9H_7BrO_4$	387.49	146.29	0.542	-367.29	26.09	-3.01	4379.97	730.46	951.00	485.36	2.073	-498.78	78.24
C_6	$C_{18}H_{14}O_7$	695.16	240.85	0.905	-524.44	39.64	-4.31	2239.76	957.30	1196.42	636.91	2.534	-811.71	95.75
C_7	$C_9H_8O_5$	356.58	134.66	0.498	-476.98	22.38	-1.91	3995.65	681.74	888.91	435.27	1.530	-645.86	73.56
C_8	$C_{10}H_9ClO_4$	404.42	155.12	0.580	-377.93	24.46	-2.53	3501.28	719.19	932.38	439.23	1.917	-555.30	77.37
C_9	$C_8H_8O_3$	276.25	113.13	0.418	-251.48	23.90	-1.56	4260.71	582.57	787.82	372.23	1.393	-433.80	91.80
C_{10}	$C_{10}H_{10}O_5$	405.84	148.75	0.554	-478.19	24.58	-1.97	3488.88	709.60	914.96	459.06	1.319	-677.97	76.44
C_{11}	$C_9H_8O_5$	355.17	134.66	0.499	-508.80	25.28	-1.17	4608.87	751.50	950.28	473.86	0.848	-665.87	87.83
C_{12}	$C_{10}H_7F_3O_4$	523.13	148.19	0.579	-913.33	22.71	-2.69	2811.36	607.02	808.77	389.91	1.941	-1111.35	55.36
C_{13}	$C_{10}H_7Cl_3O_5$	535.43	185.47	0.691	-501.51	30.15	-3.89	3191.93	813.68	1037.46	538.72	3.270	-722.47	87.64
C_{14}	$C_9H_8O_4$	338.24	128.79	0.480	-371.98	21.19	-1.85	4082.92	659.32	868.49	400.00	1.310	-513.64	71.15
C_{15}	$C_{14}H_{10}O_5$	534.51	181.35	0.619	-372.09	33.97	-3.17	4082.92	881.02	1117.60	607.53	2.310	-557.62	97.57
C_{16}	$C_{11}H_{12}O_5$	422.32	162.84	0.610	-437.95	24.27	-2.15	2775.92	662.72	876.45	431.74	1.407	-678.60	64.40
C_{17}	$C_{13}H_{14}O_6$	467.49	192.59	0.728	-540.40	31.44	-2.15	2470.27	757.37	970.44	491.69	1.332	-820.99	74.94
C_{18}	$C_{10}H_{12}O_3$	309.67	141.31	0.529	-202.82	19.28	-2.25	2976.29	558.57	770.06	335.79	1.872	-401.69	52.36
C_{19}	$C_{14}H_8O_4$	551.34	164.62	0.610	-88.50	29.26	-3.89	3501.28	788.26	1070.21	533.66	2.438	-334.59	70.54
C_{20}	$C_{21}H_{12}O_6$	827.01	246.93	0.905	-159.69	44.33	-5.98	2576.72	1083.39	1383.53	739.24	3.658	-536.03	98.16
C_{21}	$C_{11}H_7F_5O_4$	694.26	165.82	0.659	-1291.69	24.04	-3.42	2372.59	625.21	817.70	404.78	2.576	-1532.96	54.65
C_{22}	$C_{10}H_{10}O_5$	374.00	148.75	0.553	-436.74	22.07	-2.09	3131.49	634.86	851.27	407.95	1.618	-646.49	61.51
C_{23}	$C_{13}H_8F_6O_6$	800.58	203.21	0.814	-1703.58	35.09	-3.47	1985.89	746.53	936.07	500.07	2.417	-2015.15	67.44
C_{24}	$C_{11}H_{14}O_3$	356.58	155.40	0.580	-196.84	18.35	-2.78	2709.85	581.01	793.47	332.06	2.260	-427.61	54.20
C_{25}	$C_9H_7ClO_3$	339.17	135.16	0.510	-247.09	21.30	-2.67	3484.76	604.57	834.38	382.14	1.991	-377.15	58.85
C_{26}	$C_{14}H_{12}O_3$	437.41	173.91	0.645	-56.73	23.68	-3.68	2811.36	676.77	916.60	407.29	2.914	-247.72	63.54
C_{27}	$C_{11}H_{14}O_3$	325.67	155.40	0.586	-194.40	21.87	-2.67	2687.42	581.45	789.55	347.06	2.262	-422.33	54.58
C_{28}	$C_9H_5F_3O_4$	504.78	134.10	0.523	-953.57	23.02	-2.51	3538.87	653.90	848.20	417.23	1.853	-1110.72	67.40
C_{29}	$C_9H_{10}O_4$	342.00	133.09	0.492	-357.69	20.39	-1.77	3628.97	632.85	834.15	382.50	1.402	-544.75	67.47
C_{30}	$C_{17}H_{15}NO_5$	628.98	229.30	0.861	-209.55	39.36	-4.07	2379.54	908.30	1145.45	606.14	2.789	-492.80	90.81
C_{31}	$C_{15}H_{14}O_4$	503.15	193.87	0.720	-162.94	27.07	-3.80	2465.36	727.05	959.54	453.31	2.923	-412.05	68.84
C_{32}	$C_{11}H_9F_3O_5$	588.87	168.15	0.652	-1019.54	26.10	-2.81	2465.36	657.30	855.60	435.93	1.950	-1275.68	60.66
C_{33}	$C_{12}H_7F_7O_4$	865.39	183.45	0.741	-1670.05	25.38	-4.16	2029.06	643.40	828.09	419.65	3.211	-1954.57	53.95
C_{34}	$C_{18}H_{14}O_3$	599.82	210.81	0.791	73.97	30.67	-5.48	2402.92	792.25	1040.33	497.59	4.068	-150.68	74.74
C_{35}	$C_9H_9NO_3$	339.17	132.90	0.490	-168.71	22.30	-1.96	3906.25	639.67	872.95	435.48	0.711	-327.62	65.11
C_{36}	$C_8H_7ClO_3$	324.58	125.37	0.468	-273.04	20.81	-2.34	3985.56	624.98	835.06	394.28	2.047	-407.63	67.22
C_{37}	$C_{14}H_{11}ClO_3$	485.74	186.15	0.695	-78.29	27.49	-4.36	2662.52	719.18	962.28	449.73	3.568	-274.93	68.58
C_{38}	$C_{15}H_{12}O_5$	549.58	195.44	0.673	-331.85	33.66	-3.42	3191.93	834.14	1080.69	580.21	2.537	-558.25	85.52
C_{39}	$C_9H_{10}O_4$	342.00	133.09	0.492	-357.69	20.39	-1.77	3628.97	632.85	834.15	397.86	1.402	-578.60	67.47
C_{40}	$C_{15}H_{12}O_3$	485.25	183.70	0.690	-72.23	26.68	-3.74	2764.26	731.10	975.09	446.26	2.843	-248.72	70.10
C_{41}	$C_7H_6O_3$	258.84	99.04	0.310	-299.89	25.57	-1.89	6349.11	612.91	833.23	431.35	1.090	-492.40	69.89
C_{42}	$C_{11}H_{14}O_3$	325.67	155.40	0.586	-194.40	21.87	-2.67	2687.42	581.45	789.55	347.06	2.262	-422.33	54.58
C_{43}	$C_{15}H_{11}NO_3$	503.15	189.38	0.728	75.24	27.39	-4.03	2445.89	806.71	1052.53	496.07	2.786	-114.95	76.90
C_{44}	$C_{13}H_{18}O_3$	419.49	183.58	0.685	-182.44	20.01	-3.73	2256.81	626.33	836.17	339.60	3.039	-474.17	58.26
C_{45}	$C_{17}H_{18}O_4$	566.99	222.05	0.826	-148.54	28.73	-4.75	2069.88	772.37	1000.99	460.85	3.702	-458.61	72.90

Table 3. Physicochemical properties and the elliptic Dharwad index for the studied compounds (n = 89), Part II.

Compound	Formula	ED	McVol	V_c	$\Delta_f G^\circ$	$\Delta_{\text{fus}} H^\circ$	$\log_{10}(W_S)$	P_c	T_{boil}	T_c	T_{fus}	$\log P_{\text{oct/wat}}$	$\Delta_f H^\circ_{\text{gas}}$	$\Delta_{\text{vap}} H^\circ$
C_{46}	$C_9H_{10}O_4$	342.93	133.09	0.492	-357.69	20.39	-2.14	3628.97	632.85	834.15	397.86	1.402	-544.75	67.47
C_{47}	$C_9H_8O_4$	338.24	128.79	0.480	-371.98	21.19	-1.85	4082.92	659.32	868.49	413.04	1.310	-513.64	71.15
C_{48}	$C_{14}H_{10}Cl_2O_3$	534.99	198.39	0.744	-99.85	31.30	-5.05	2525.19	761.59	1007.60	492.17	4.221	-302.14	73.63
C_{49}	$C_{13}H_{10}O_3$	420.00	159.82	0.537	-105.14	26.08	-3.15	3862.67	707.11	962.79	314.75	2.611	-260.70	71.25
C_{50}	$C_{12}H_9F_5O_5$	760.00	185.78	0.734	-1397.90	27.43	-3.54	2102.27	675.49	865.86	450.80	2.585	-1697.29	59.95
C_{51}	$C_{10}H_{10}O_4$	355.65	142.88	0.535	-331.74	20.88	-2.03	3191.93	612.44	831.50	385.72	1.398	-514.27	59.10
C_{52}	$C_{14}H_{11}ClO_3$	486.67	186.15	0.695	-78.29	27.49	-4.36	2662.52	719.18	962.28	449.73	3.568	-274.93	68.58
C_{53}	$C_{10}H_{12}O_3$	309.67	141.31	0.529	-202.82	19.28	-2.25	2976.29	534.65	770.06	335.79	1.872	-401.69	52.36
C_{54}	$C_{10}H_5F_5O_4$	675.91	151.73	0.605	-1331.93	24.35	-3.24	2928.17	672.09	858.93	432.10	2.488	-1532.33	66.70
C_{55}	$C_{14}H_{10}F_2O_3$	534.06	177.45	0.681	-465.61	29.07	-4.34	2485.07	685.27	905.92	433.51	3.193	-662.88	63.23
C_{56}	$C_{15}H_{11}ClO_3$	533.58	195.94	0.739	-93.79	30.49	-4.43	2619.09	773.51	1020.33	488.70	3.496	-275.93	75.15
C_{57}	$C_{14}H_{12}O_4$	485.74	179.78	0.612	-211.35	29.47	-3.23	3314.37	757.39	1004.09	519.01	2.620	-425.03	76.55
C_{58}	$C_{10}H_{10}O_4$	356.58	142.88	0.535	-331.74	20.88	-2.03	3191.93	612.44	831.50	385.72	1.398	-514.27	59.10
C_{59}	$C_{15}H_8F_{10}O_6$	1142.85	238.47	0.976	-2460.30	37.76	-4.94	1504.65	782.91	966.28	529.81	3.687	-2858.37	66.04
C_{60}	$C_{15}H_{12}O_3$	485.25	183.70	0.690	-72.23	26.68	-4.22	2764.26	731.10	975.09	446.26	3.108	-248.72	70.10
C_{61}	$C_{13}H_9ClO_3$	468.32	172.06	0.587	-126.70	29.89	-3.79	3624.61	749.52	1007.84	515.43	3.265	-287.91	76.30
C_{62}	$C_{14}H_{11}NO_5$	550.99	191.33	0.728	-30.81	34.66	-4.33	2802.44	833.59	1091.42	563.42	2.823	-269.95	80.79
C_{63}	$C_{12}H_{16}O_3$	374.00	169.49	0.635	-188.42	20.94	-3.20	2458.04	603.89	812.91	343.33	2.651	-448.25	56.42
C_{64}	$C_{11}H_5F_7O_4$	847.05	169.36	0.685	-1710.29	25.69	-3.97	2462.92	690.28	871.19	446.97	3.123	-1953.94	65.99
C_{65}	$C_{15}H_{14}O_3$	486.67	188.00	0.702	-57.94	25.89	-4.15	2507.52	704.63	940.44	431.08	3.223	-279.83	66.43
C_{66}	$C_{12}H_{16}O_3$	372.58	169.49	0.635	-188.42	20.94	-2.85	2458.04	603.89	812.91	343.33	2.508	-448.25	56.42
C_{67}	$C_{16}H_{12}O_6$	682.82	204.54	0.757	-300.92	36.04	-4.13	2640.67	888.82	1149.83	625.70	2.456	-663.25	81.14
C_{68}	$C_9H_{10}O_3$	293.67	127.22	0.473	-211.24	16.69	-1.83	3314.37	521.20	750.72	324.52	1.482	-381.05	50.13
C_{69}	$C_{11}H_{10}O_5$	418.56	158.54	0.598	-452.24	25.07	-2.22	3076.16	689.19	910.86	446.92	1.315	-647.49	68.08
C_{70}	$C_{10}H_{10}O_4$	357.07	142.88	0.546	-311.97	21.18	-2.15	3177.55	612.21	827.41	390.31	1.433	-498.74	59.74
C_{71}	$C_{20}H_{18}O_7$	727.16	269.03	1.018	-507.60	44.82	-4.16	1882.17	1003.06	1240.69	659.45	2.619	-852.99	100.20
C_{72}	$C_{18}H_{14}O_7$	631.48	240.85	0.927	-465.64	41.02	-3.32	2287.14	946.88	1179.94	621.05	1.839	-757.71	95.70
C_{73}	$C_{10}H_7F_3O_4$	523.13	148.19	0.579	-913.33	22.71	-2.69	2811.36	607.02	808.77	389.91	1.941	-1111.35	55.36
C_{74}	$C_{21}H_{18}O_4$	662.89	254.65	0.948	-0.01	36.65	-5.91	1959.60	891.01	1137.48	547.35	4.493	-299.36	84.47
C_{75}	$C_{13}H_{18}O_3$	357.67	183.58	0.698	-177.56	27.05	-3.51	2222.89	627.21	829.16	369.60	3.042	-463.61	59.04
C_{76}	$C_{14}H_{10}BrFO_3$	534.99	193.18	0.726	-256.48	31.27	-5.17	2793.56	752.16	992.93	492.72	3.816	-440.44	70.48
C_{77}	$C_{12}H_{12}O_5$	468.75	172.63	0.653	-453.45	27.27	-2.76	2729.71	717.05	935.93	470.71	1.740	-679.60	70.96
C_{78}	$C_{10}H_{12}O_4$	325.67	147.18	0.548	-339.64	23.37	-1.52	3299.15	650.75	848.60	396.61	0.844	-553.92	69.04
C_{79}	$C_{15}H_{14}O_3$	485.74	188.00	0.702	-57.94	25.89	-4.15	2507.52	704.63	940.44	431.08	3.223	-279.83	66.43
C_{80}	$C_{18}H_{12}O_6$	615.48	230.68	0.889	-280.42	40.03	-4.08	2445.89	928.62	1168.44	593.74	2.379	-508.27	93.25
C_{81}	$C_{13}H_9F_7O_5$	931.13	203.41	0.815	-1776.26	28.77	-4.28	1813.86	693.68	877.67	465.67	3.220	-2118.90	59.25
C_{82}	$C_{19}H_{16}O_6$	631.48	249.07	0.966	-352.22	42.42	-4.65	2123.64	947.34	1179.79	610.09	2.993	-646.13	95.52
C_{83}	$C_{16}H_{14}O_5$	569.34	209.53	0.781	-283.44	31.26	-3.92	2386.52	803.80	1037.51	514.51	2.701	-545.27	77.81
C_{84}	$C_{13}H_{16}O_5$	422.00	191.02	0.722	-411.48	29.84	-2.37	2322.54	703.50	910.34	441.76	1.805	-708.41	68.19
C_{85}	$C_{13}H_{10}O_3$	420.00	159.82	0.591	-96.97	23.99	-3.17	3538.87	723.65	951.31	434.61	3.177	-247.09	75.58
C_{86}	$C_9H_{10}O_4$	342.93	133.09	0.492	-357.69	20.39	-1.77	3628.97	632.85	834.15	397.86	1.402	-544.75	67.47
C_{87}	$C_{14}H_{12}O_3$	468.32	173.91	0.594	-106.35	28.28	-3.58	3380.21	734.97	985.71	496.78	2.920	-292.81	74.14
C_{88}	$C_{11}H_{14}O_4$	341.67	161.27	0.604	-299.40	23.06	-1.76	2640.67	603.87	809.83	369.29	1.498	-554.55	56.99
C_{89}	$C_{11}H_{14}O_3$	356.58	155.40	0.580	-196.84	18.35	-2.78	2709.85	581.01	793.47	332.06	2.260	-427.61	54.20

3.2. Pairwise correlation of ED with the physicochemical properties

Before fitting predictive models, we examined the pairwise Pearson correlation between the elliptic Dharwad index and each physicochemical response; see Table 4. The strongest positive associations were observed for the volumetric descriptors V_c ($r = 0.789$) and McVol ($r = 0.736$), indicating that ED tracks molecular size and bulk-related structural variation rather well. A comparatively strong positive correlation was also found for $\Delta_{\text{fus}}H^\circ$ ($r = 0.671$), while T_{fus}, $\log P_{\text{oct/wat}}$, T_{boil}, and T_c showed moderate positive associations.

On the negative side, the largest inverse correlations were found for $\log_{10}(W_S)$ ($r = -0.714$), $\Delta_f H^\circ_{\text{gas}}$ ($r = -0.709$), $\Delta_f G^\circ$ ($r = -0.658$), and P_c ($r = -0.640$). These patterns suggest that larger ED values tend to be associated with lower water solubility, more negative formation energies, and lower critical pressure within the present chemical family. By contrast, $\Delta_{\text{vap}}H^\circ$ displayed only a weak positive association ($r = 0.285$), indicating that this endpoint is only weakly aligned with ED at the pairwise level.

Table 4. Pearson correlation coefficients between the elliptic Dharwad index and the physicochemical endpoints ($n = 89$).

Endpoint	r	Direction
V_c	0.789	Positive
McVol	0.736	Positive
$\log_{10}(W_S)$	-0.714	Negative
$\Delta_f H^\circ_{\text{gas}}$	-0.709	Negative
$\Delta_{\text{fus}}H^\circ$	0.671	Positive
$\Delta_f G^\circ$	-0.658	Negative
P_c	-0.640	Negative
T_{fus}	0.622	Positive
$\log P_{\text{oct/wat}}$	0.594	Positive
T_{boil}	0.592	Positive
T_c	0.531	Positive
$\Delta_{\text{vap}}H^\circ$	0.285	Positive

Overall, these correlations suggest that ED is most informative for volumetric and size-related properties, while its relationship with some thermodynamic responses is weaker or more indirect. This supports the use of ED as a compact exploratory descriptor, while also indicating that not all endpoints should be expected to show equally strong univariate predictive behavior. A full correlation heatmap for ED and all physicochemical endpoints is provided in Figure 4.

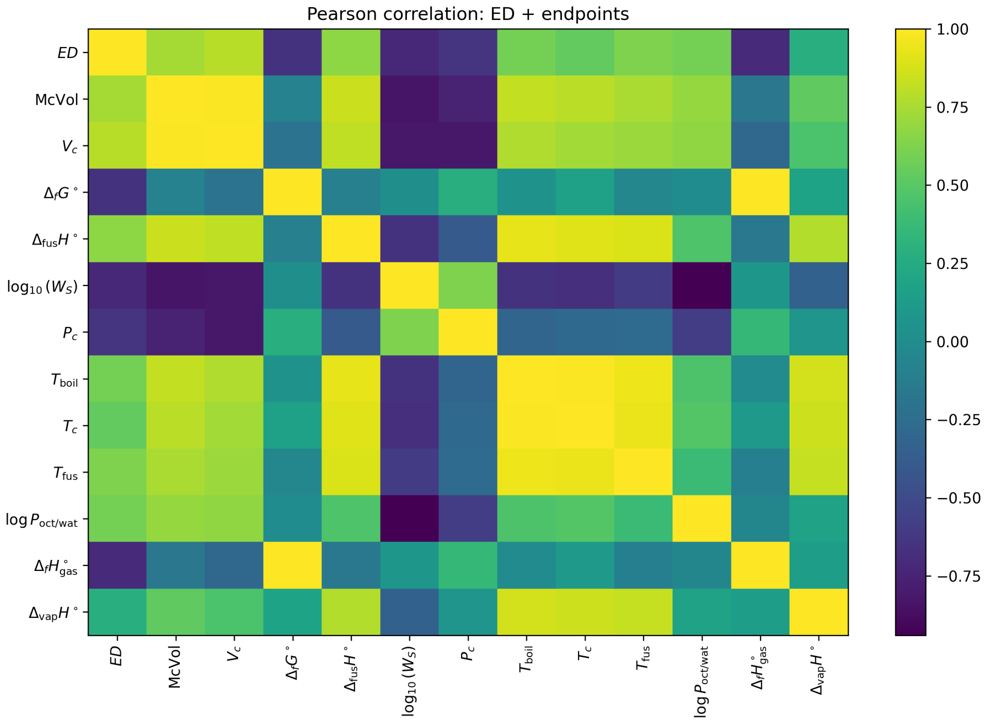

Figure 4. Correlation heatmap for the elliptic Dharwad index and the physicochemical endpoints considered in the present QSPR study.

3.3. Modeling strategy

The predictive utility of *ED* was evaluated in a deliberately low-dimensional QSPR setting in which each endpoint was modeled using *ED* as the sole descriptor. Alongside interpretable baseline regressions, namely linear ordinary least squares (OLS), quadratic OLS, and log-linear OLS based on $\log(1 + ED)$, we also screened several more flexible nonlinear learners, including K-nearest neighbors, support vector regression with a Radial Basis Function (RBF) kernel, tree-based ensemble methods, and gradient boosting models when the relevant libraries were available in the computational environment. The complete computational workflow used for descriptor calculation, model screening, cross-validation, external test evaluation, and diagnostic analyses is provided in Supplementary 2.

The compounds were divided into training and external test subsets by a Kennard–Stone split performed in the one-dimensional *ED* space, using an approximate 80:20 partition. Internal robustness was assessed on the training set by repeated five-fold cross-validation. The model's quality was summarized by the Q^2_{CV}, R^2_{test}, root mean square error (RMSE), and mean absolute error (MAE). Since the analysis is based on a single topological descriptor and a relatively small dataset, the resulting models are interpreted as exploratory screening models rather than final predictive tools. A single scalar degree descriptor cannot encode all size-independent electronic, functional-group, stereochemical, or three-dimensional effects. Future models should therefore combine *ED* with complementary constitutional, electronic, and physicochemical descriptors and evaluate the resulting feature sets on larger, scaffold-diverse datasets.

3.4. Predictive behavior of ED

Across the expanded ED-only model screen, the most balanced predictive behavior was observed for V_c, McVol, and $\log_{10}(W_S)$. The endpoint-wise results of the expanded ED-only screening are summarized in Table 5. The strongest overall compromise between internal and external validation was obtained for V_c, for which a log-linear model based on $\log(1 + ED)$ achieved $Q^2_{\mathrm{CV}} = 0.548$ and $R^2_{\mathrm{test}} = 0.636$. A similar but slightly weaker pattern was found for McVol, with $Q^2_{\mathrm{CV}} = 0.499$ and $R^2_{\mathrm{test}} = 0.514$. Water solubility also displayed a meaningful ED-dependent signal, yielding the highest cross-validated robustness among all endpoints ($Q^2_{\mathrm{CV}} = 0.568$), together with moderate external predictive performance ($R^2_{\mathrm{test}} = 0.450$).

A moderate exploratory signal was further observed for $\Delta_{\mathrm{fus}}H^{\circ}$, T_{boil}, and T_{fus}, whereas T_c and $\log P_{\mathrm{oct/wat}}$ remained weaker. By contrast, $\Delta_f G^{\circ}$, $\Delta_f H^{\circ}_{\mathrm{gas}}$, P_c, and $\Delta_{\mathrm{vap}}H^{\circ}$ showed negative Q^2_{CV} values despite moderate or, in some cases, relatively high external test R^2 values. This mismatch points to substantial split sensitivity and possible overfitting, so these endpoints should not be interpreted as reliable standalone predictive successes of the elliptic Dharwad index.

Overall, the expanded screening supports the elliptic Dharwad index as a compact exploratory descriptor with its clearest utility for volumetric and related bulk physicochemical properties. At the same time, the results indicate that more demanding thermodynamic responses are likely to require richer multidescriptor representations.

Representative observed-versus-predicted plots for the two most balanced ED-based models, namely V_c and McVol, are presented in Figure 5. The corresponding supplementary plots are provided in Figure 6. Additional observed-versus-predicted plots for other endpoints are provided in Figures 7 and 8, while repeated cross-validation stability plots, residual diagnostics, permutation tests, and Williams plots are collected in Figures 9–19. The distribution of ED values and the descriptor space coverage induced by the Kennard–Stone split are shown in Figure 20.

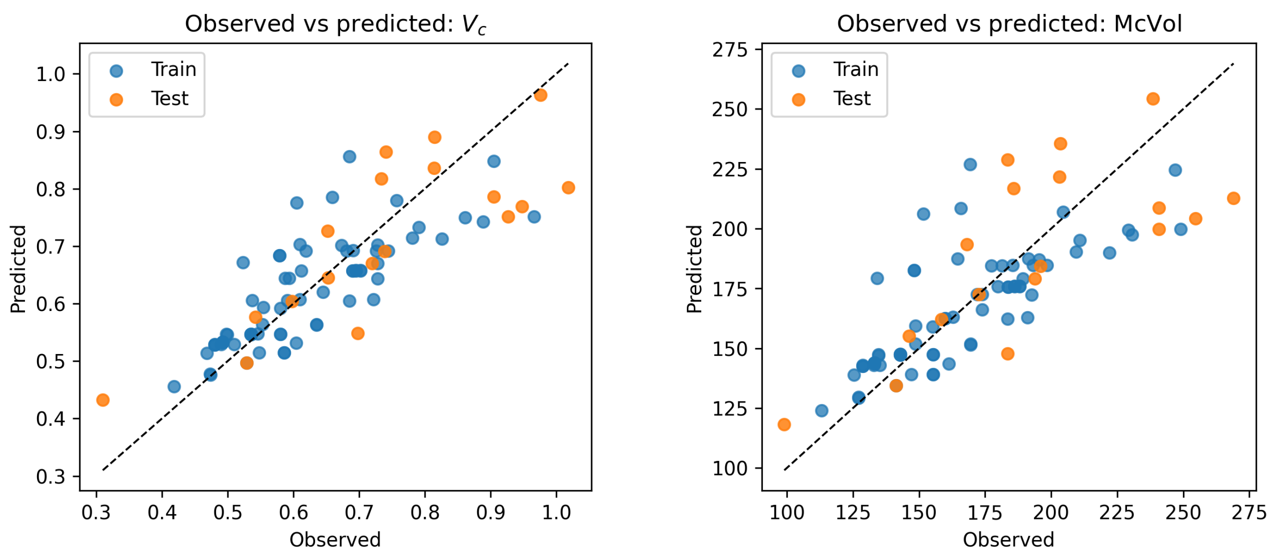

(a) V_c **(b)** McVol

Figure 5. Observed-versus-predicted plots for the two most balanced ED-based univariate QSPR models: (a) Critical volume (V_c) and (b) McGowan characteristic volume (McVol).

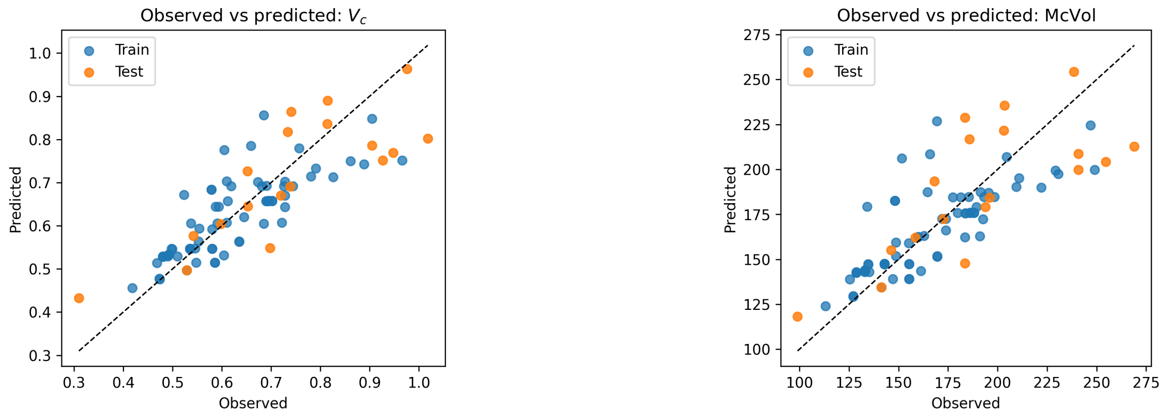

(a) Critical volume, V_c. **(b)** McGowan characteristic volume, McVol.

Figure 6. Observed-versus-predicted plots for the two most balanced ED-based QSPR models.

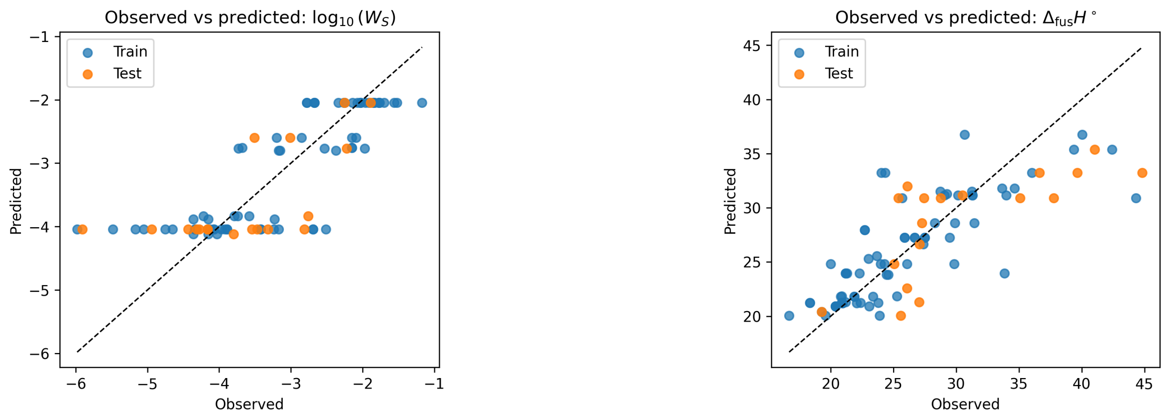

(a) Water solubility, $\log_{10}(W_S)$. **(b)** Standard enthalpy of fusion, $\Delta_{\text{fus}}H^\circ$.

Figure 7. Observed-versus-predicted plots for additional endpoints showing moderate ED-based signals.

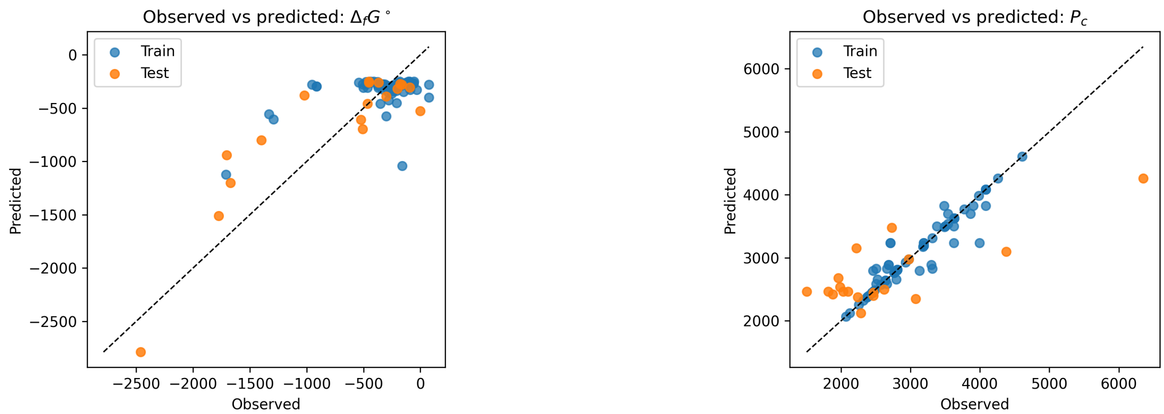

(a) Standard Gibbs energy of formation, $\Delta_f G^\circ$. **(b)** Critical pressure, P_c.

Figure 8. Observed-versus-predicted plots for endpoints whose external test performance is accompanied by unstable cross-validation behavior.

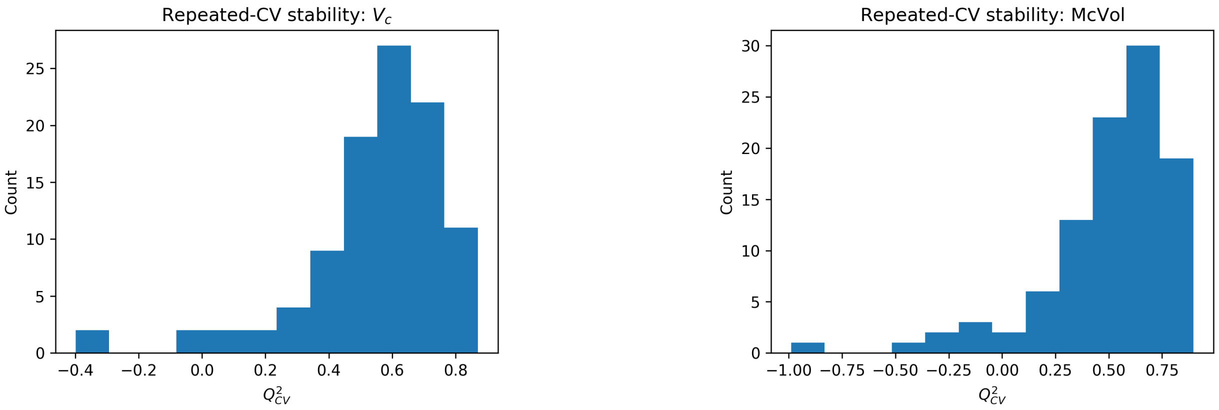

(a) V_c.

(b) McVol.

Figure 9. Repeated cross-validation stability plots for the strongest ED-based QSPR models.

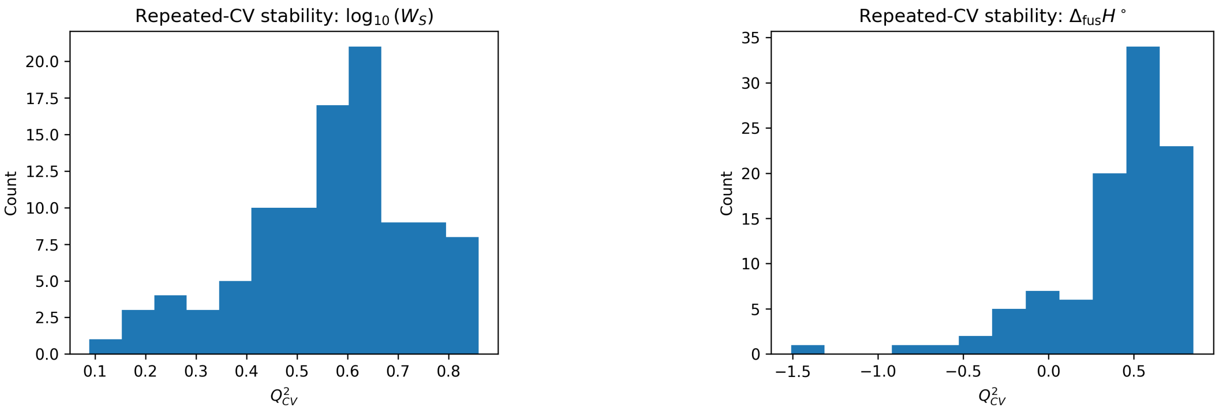

(a) $\log_{10}(W_S)$.

(b) $\Delta_{\mathrm{fus}}H^\circ$.

Figure 10. Repeated cross-validation stability plots for additional endpoints with moderate ED-based signals.

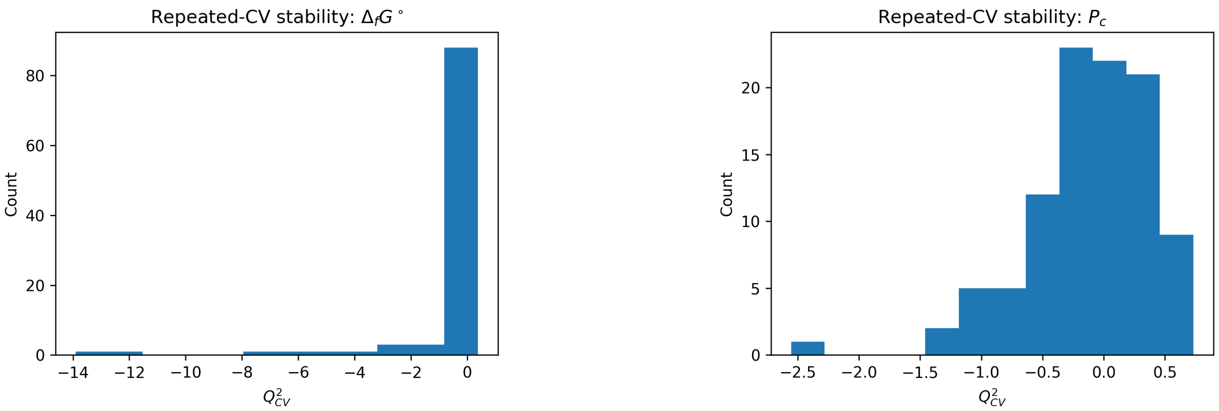

(a) $\Delta_f G^\circ$.

(b) P_c.

Figure 11. Repeated cross-validation stability plots for endpoints exhibiting marked split sensitivity.

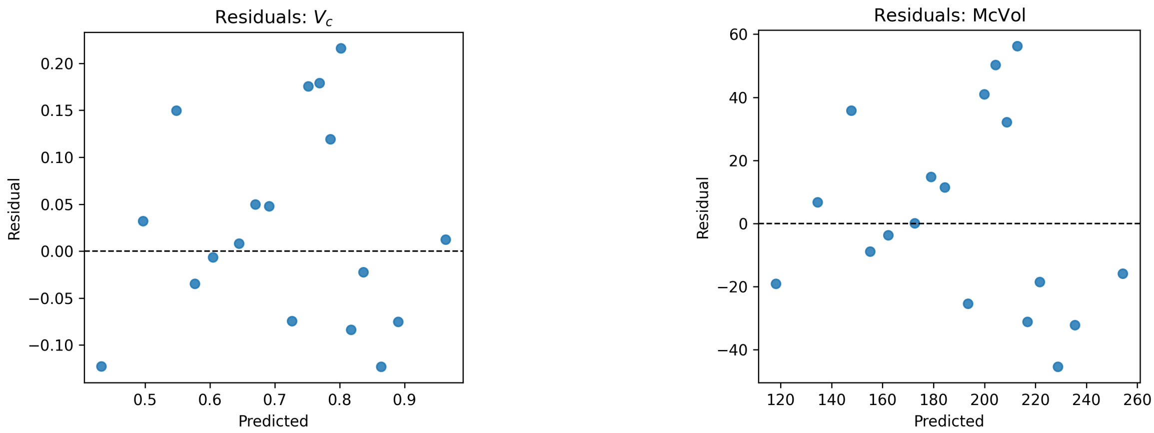

(a) V_c.　**(b)** McVol.

Figure 12. Residual plots for the strongest ED-based QSPR models.

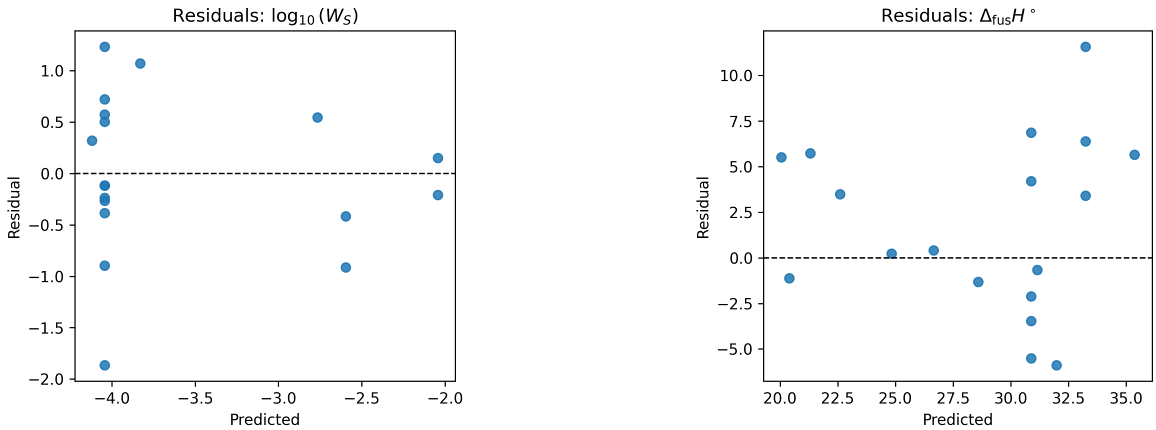

(a) $\log_{10}(W_S)$.　**(b)** $\Delta_{\text{fus}}H^\circ$.

Figure 13. Residual plots for additional endpoints with moderate ED-based predictive signals.

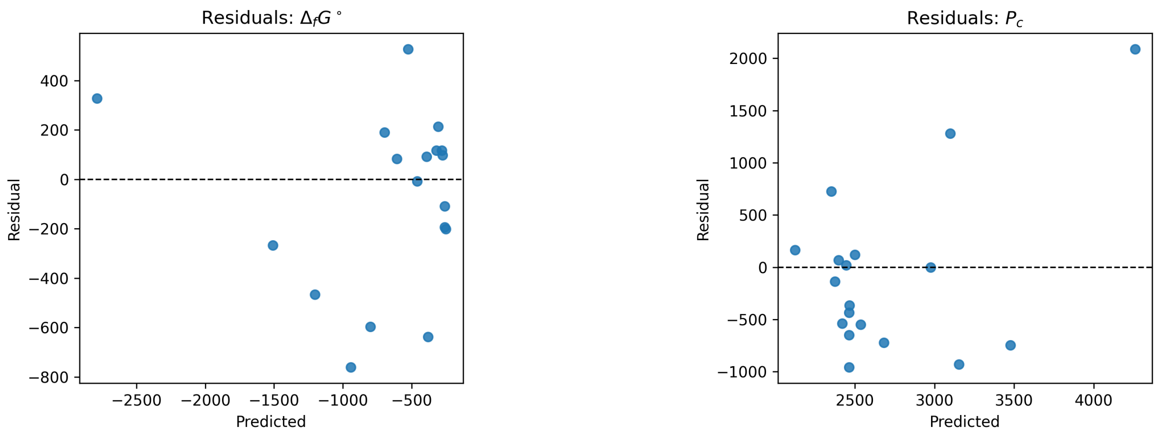

(a) $\Delta_f G^\circ$.　**(b)** P_c.

Figure 14. Residual plots for endpoints with unstable validation behavior.

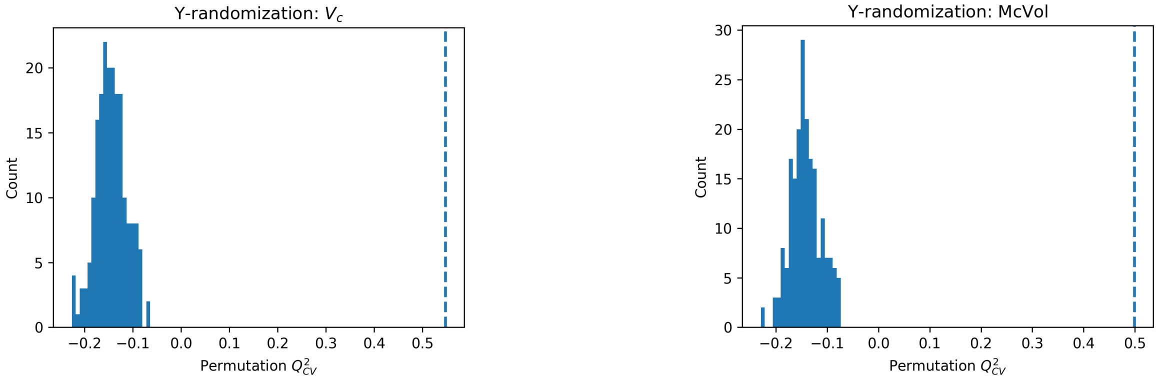

(a) V_c. **(b)** McVol.

Figure 15. Permutation test diagnostics for the strongest ED-based QSPR models.

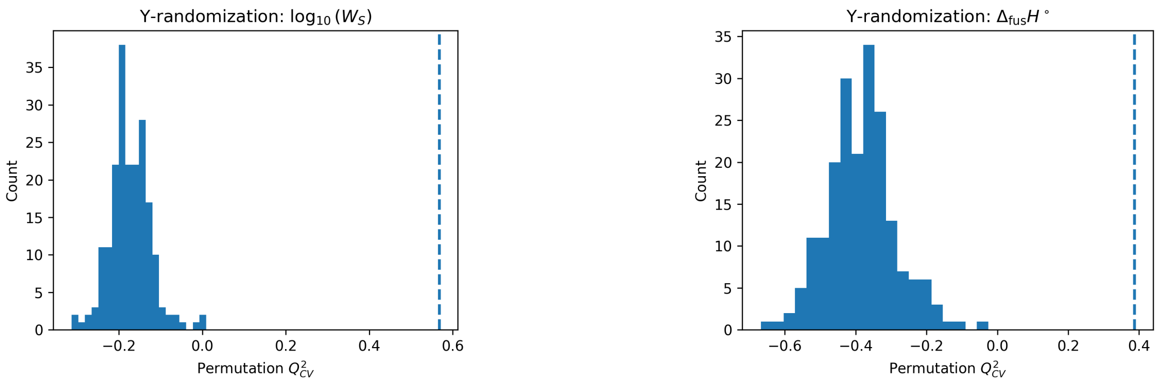

(a) $\log_{10}(W_S)$. **(b)** $\Delta_{\text{fus}}H^\circ$.

Figure 16. Permutation test diagnostics for additional endpoints with moderate ED-based signal.

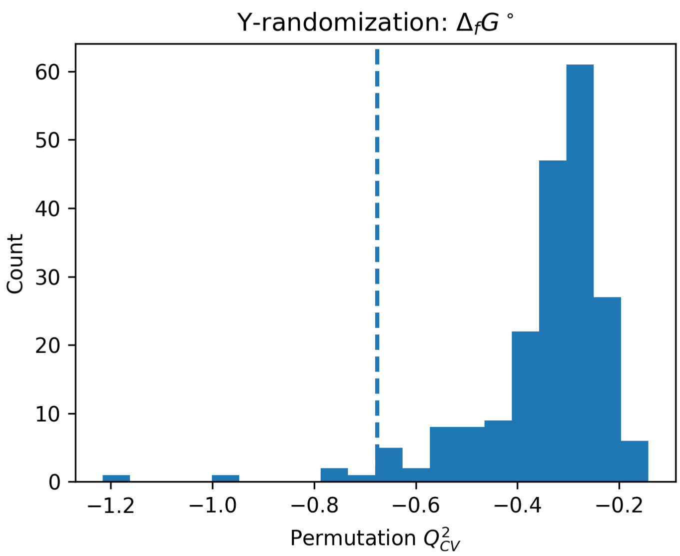

Figure 17. Permutation test diagnostic for $\Delta_f G^\circ$, illustrating the gap between nominal external performance and validation stability.

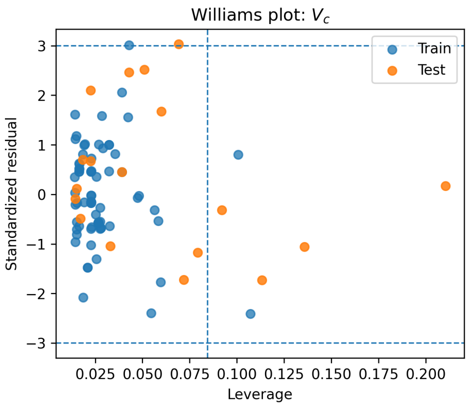

(a) V_c.

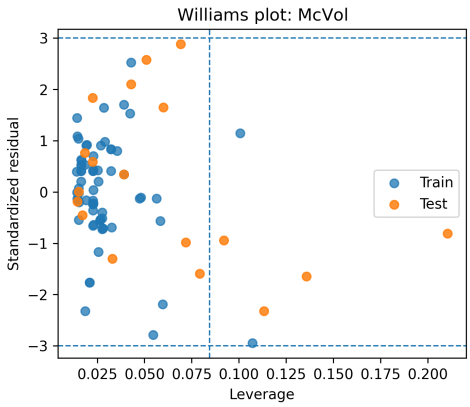

(b) McVol.

Figure 18. Williams plots for the two most balanced ED-based QSPR models.

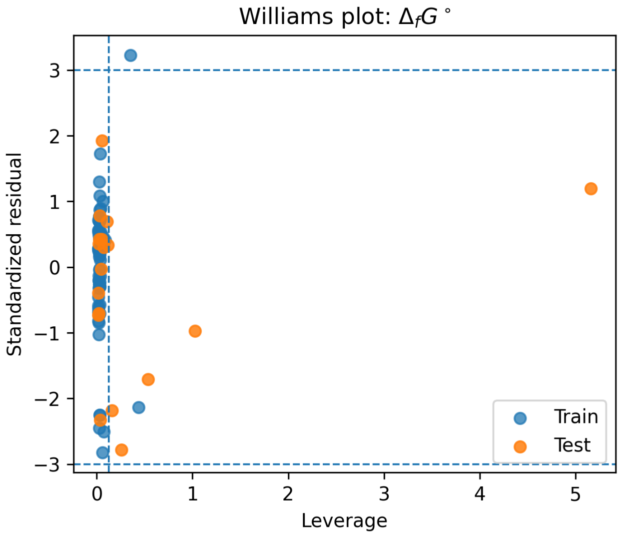

Figure 19. Williams plot for $\Delta_f G^\circ$.

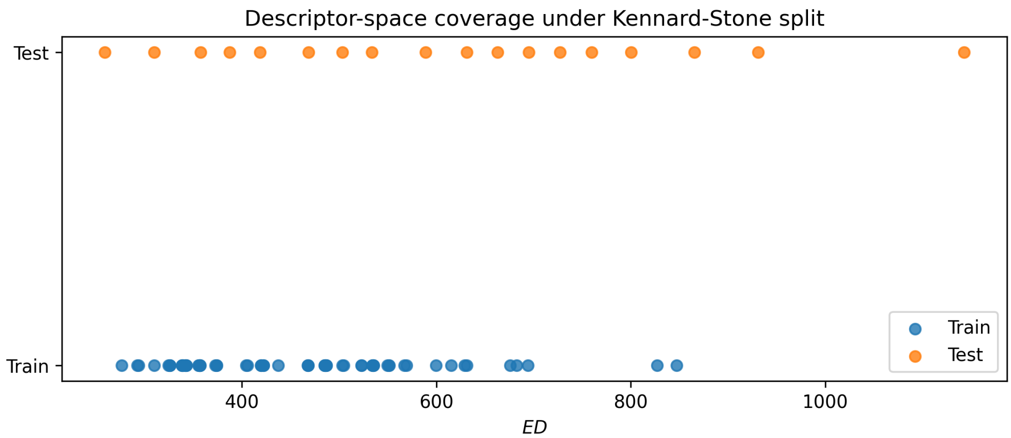

Figure 20. Distribution and coverage of the elliptic Dharwad index across the 89-compound dataset used for the exploratory QSPR analysis.

Table 5. Expanded univariate QSPR screening results for the elliptic Dharwad index. Here, r is the Pearson correlation between ED and the endpoint, Q^2_{CV} is the mean repeated five-fold cross-validated coefficient of determination on the training set, and R^2_{test} is the coefficient of determination on the external test set.

Endpoint	r	Best model	Q^2_{CV}	R^2_{test}	$\mathrm{RMSE}_{\mathrm{test}}$	$\mathrm{MAE}_{\mathrm{test}}$
McVol	0.736	Log-linear $\log(1+ED)$+OLS	0.499	0.514	29.653	24.907
V_c	0.789	Log-linear $\log(1+ED)$+OLS	0.548	0.636	0.106	0.085
$\Delta_f G^\circ$	-0.658	Quadratic OLS	-0.676	0.748	352.930	278.030
$\Delta_{\mathrm{fus}} H^\circ$	0.671	K-nearest neighbors	0.387	0.446	4.968	4.089
$\log_{10}(W_S)$	-0.714	LightGBM	0.568	0.450	0.739	0.586
P_c	-0.640	ExtraTrees	-0.117	0.503	774.197	582.916
T_{boil}	0.592	K-nearest neighbors	0.392	0.419	93.661	71.217
T_c	0.531	K-nearest neighbors	0.389	0.297	114.403	90.832
T_{fus}	0.622	K-nearest neighbors	0.352	0.379	66.333	54.504
$\log P_{\mathrm{oct/wat}}$	0.594	LightGBM	0.398	0.250	0.739	0.616
$\Delta_f H^\circ_{\mathrm{gas}}$	-0.709	Quadratic OLS	-0.456	0.779	351.331	266.321
$\Delta_{\mathrm{vap}} H^\circ$	0.285	SVR (RBF)	-0.097	0.322	11.523	9.215

4. Conclusions

In this paper, we introduced and investigated the elliptic Dharwad index

$$ED(\mathcal{I}) = \sum_{uv\in E(\mathcal{I})} (d(u) + d(v))\sqrt{d(u)^3 + d(v)^3},$$

as a new degree-based edge invariant that strengthens the effect of degree heterogeneity through a cubic degree kernel. The study shows that this index is both mathematically tractable and structurally informative, with a behavior that is well suited to graph operations, extremal analysis, and exploratory chemical applications.

More specifically, ED preserves the cubic Dharwad kernel while adding the elliptic degree-sum prefactor; compared with the elliptic Sombor index, it replaces the quadratic radial term by a cubic one. This combined weighting produces faster growth on high-degree edges and stronger discrimination of unequal endpoint degrees at a fixed degree sum.

On the theoretical side, we established sharp two-sided bounds for the join $\mathcal{I}+\mathcal{J}$, the corona product $\mathcal{I}\odot\mathcal{J}$, the Cartesian product $\mathcal{I}\square\mathcal{J}$, and the tensor product $\mathcal{I}\otimes\mathcal{J}$, together with explicit equality characterizations. In the regular case, these results reduce to compact closed formulas, showing that the general bounds are exact on broad and important graph classes. We also derived explicit closed forms for several standard constructions, including the joins and coronas of paths, cycles, and complete graphs, thereby illustrating how degree-based edge partitions can be used to compute ED effectively.

We further addressed extremal aspects of the index. In particular, we proved that ED is strictly increasing under edge addition, which makes it suitable for extremal comparisons through graph densification. Using this monotonicity together with structural decomposition arguments, we obtained girth-based sharp lower bounds for unicyclic graphs and extended these results to connected graphs with a prescribed girth, with complete characterization of the extremal cases. We also established a best possible upper bound for graphs of fixed order with a prescribed number of pendant vertices, and showed that the unique extremal graph is $K_{s,p}$.

To complement the theoretical development, we examined the descriptor in a univariate QSPR setting on a Cheméo-based dataset of 89 unique aromatic carboxylic acid, ester, and related benzenoid compounds. This application indicates that the elliptic Dharwad index carries its clearest standalone signal for volumetric and size-related properties, especially V_c, McVol, and, to a lesser extent, $\log_{10}(W_S)$. At the same time, the results show that several thermodynamic endpoints are only moderately captured or remain unstable under validation. Accordingly, the present QSPR analysis should be viewed as an exploratory screening study that demonstrates the descriptive value of ED, rather than as a final predictive modeling framework.

Overall, the results show that the elliptic Dharwad index combines three desirable features: It admits exact evaluation on many structured graph families, it satisfies sharp extremal principles under classical graph constraints, and it displays meaningful structure property signals in chemical graph applications. These features support ED as a useful addition to the family of degree-based topological indices.

Several natural directions remain open. It would be worthwhile to compute ED for further graph classes, develop Nordhaus–Gaddum type relations and sharper inequalities linking ED with classical indices, study efficient algorithms for evaluating ED on large-scale graphs, and investigate multidescriptor QSPR or Quantitative Structure Activity Relationship (QSAR) frameworks in which ED is combined with complementary topological or physicochemical descriptors.

Author contributions

Conceptualization: S.W., M.A.; methodology: M.A.; validation: S.W.; investigation: M.A.; data analysis and curation: M.A.; resources: S.W.; writing-original draft: M.A.; writing-review and editing: S.W. All authors have read and agreed to the published version of the manuscript.

Use of Generative-AI tools declaration

The authors declare that the use of AI tools was limited to language editing and grammatical refinement. All scientific content, proofs, results, and conclusions were developed and independently verified by the authors, who take full responsibility for the work.

Funding

The authors gratefully acknowledge the Deanship of Scientific Research (DSR) at King Abdulaziz University, Jeddah, Saudi Arabia, for funding this project under grant No. (IPP: 940-247-2026) and for providing technical support.

Conflict of interest

The authors declare no conflicts of interest.

References

1. I. Gutman, N. Trinajstić, Graph theory and molecular orbitals. Total φ-electron energy of alternant hydrocarbons, *Chem. Phys. Lett.*, **17** (1972), 535–538. https://doi.org/10.1016/0009-2614(72)85099-1

2. M. Randić, Characterization of molecular branching, *J. Am. Chem. Soc.*, **97** (1975), 6609–6615. https://doi.org/10.1021/ja00856a001

3. I. Gutman, Degree-based topological indices, *Croat. Chem. Acta*, **86** (2013), 351–361. https://doi.org/10.5562/cca2294

4. S. Nikolić, G. Kovačević, A. Miličević, N. Trinajstić, The Zagreb indices 30 years after, *Croat. Chem. Acta*, **76** (2003), 113–124.

5. I. Gutman, K. C. Das, The first Zagreb index 30 years after, *MATCH Commun. Math. Comput. Chem.*, **50** (2004), 83–92.

6. K. Xu, M. Liu, K. C. Das, I. Gutman, B. Furtula, A survey on Zagreb indices, *MATCH Commun. Math. Comput. Chem.*, **78** (2017), 17–56.

7. K. C. Das, Sharp bounds for Zagreb indices, *Chem. Phys. Lett.*, **511** (2011), 452–454.

8. B. Borovićanin, K. C. Das, B. Furtula, I. Gutman, Bounds for Zagreb indices, *MATCH Commun. Math. Comput. Chem.*, **78** (2017), 17–100.

9. B. Furtula, I. Gutman, A forgotten topological index, *J. Math. Chem.*, **53** (2015), 1184–1190. https://doi.org/10.1007/s10910-015-0480-z

10. A. Gagarin, K. Chellali, O. D. Makinde, Generalized Zagreb indices and their applications, *Discrete Math. Lett.*, **8** (2022), 30–38.

11. X. Zhu, Q. Huang, H. Deng, New generalizations of the Zagreb indices and their extremal properties, *J. Math. Chem.*, **58** (2020), 1095–1114.

12. G. H. Shirdel, H. Rezapour, A. M. Sayadi, The hyper-Zagreb index of graph operations, *Iran. J. Math. Chem.*, **4** (2013), 213–220.

13. B. Basavanagoud, S. Patil, A note on hyper-Zagreb index of graph operations, *Iran. J. Math. Chem.*, **7** (2016), 89–92.

14. K. Pattabiraman, M. Vijayaragavan, Hyper Zagreb indices and its coindices of graphs, *Bull. Int. Math. Virt. Inst.*, **7** (2017), 31–41.

15. I. Gutman, Geometric approach to degree-based topological indices: Sombor indices, *MATCH Commun. Math. Comput. Chem.*, **86** (2021), 11–16.

16. R. Cruz, I. Gutman, J. Rada, Sombor index of chemical graphs, *Appl. Math. Comput.*, **399** (2021), 126018. https://doi.org/10.1016/j.amc.2021.126018

17. K. C. Das, A. S. Çevik, I. N. Cangul, Y. Shang, On Sombor index, *Symmetry*, **13** (2021), 140. https://doi.org/10.3390/sym13010140

18. I. Redžepović, Chemical applicability of Sombor indices, *J. Serb. Chem. Soc.*, **86** (2021), 445–457. https://doi.org/10.2298/JSC201215006R

19. Z. Wang, Y. Mao, Y. Li, B. Furtula, On relations between Sombor and other degree-based indices, *J. Appl. Math. Comput.*, **68** (2022), 1–17. https://doi.org/10.1007/s12190-021-01516-x

20. N. Ghanbari, S. Alikhani, Sombor index of certain graphs, *Iranian J. Math. Chem.*, **12** (2021), 27–37. https://doi.org/10.22052/ijmc.2021.242106.1547

21. H. Chen, W. Li, J. Wang, Extremal values on the Sombor index of trees, *MATCH Commun. Math. Comput. Chem.*, **87** (2022), 23–49. https://doi.org/10.46793/match.87-1.023C

22. H. Deng, Z. Tang, R. Wu, Molecular trees with extremal values of Sombor indices, *Int. J. Quantum Chem.*, **121** (2021), e26622. https://doi.org/10.1002/qua.26622

23. S. Li, Z. Wang, M. Zhang, On the extremal Sombor index of trees with a given diameter, *Appl. Math. Comput.*, **416** (2022), 126731. https://doi.org/10.1016/j.amc.2021.126731

24. V. R. Kulli, Dharwad indices, *Int. J. Eng. Sci. Res. Technol.*, **10** (2021), 17–21.

25. V. R. Kulli, I. Gutman, B. Furtula, I. Redžepovic, Sombor, Nirmala, Dharwad, and F-Sombor indices–A comparative study, *SSRG Int. J. Appl. Chem.*, **10** (2023), 7–10. https://doi.org/10.14445/23939133/IJAC-V10I2P102

26. I. Gutman, B. Furtula, M. S. Oz, Geometric approach to vertex-degree-based topological indices–Elliptic Sombor index, theory and application, *Int. J. Quantum Chem.*, **124** (2024), e27346. https://doi.org/10.1002/qua.27346

27. C. Espinal, I. Gutman, J. Rada, Elliptic Sombor index of chemical graphs, *Commun. Comb. Optim.*, **10** (2025), 989–999.

28. N. De, S. M. A. Nayeem, A. Pal, The F-coindex of some graph operations, *SpringerPlus*, **5** (2016), 221. https://doi.org/10.1186/s40064-016-1864-7

29. S. Akhter, M. Imran, Z. Raza, Bounds for the general sum-connectivity index of composite graphs, *J. Inequal. Appl.*, **2017** (2017), 76. https://doi.org/10.1186/s13660-017-1350-y

30. M. Imran, S. Baby, H. M. A. Siddiqui, M. K. Shafiq, On the bounds of degree-based topological indices of the Cartesian product of F-sum of connected graphs, *J. Inequal. Appl.*, **2017** (2017), 305. https://doi.org/10.1186/s13660-017-1579-5

31. S. Oğuz Ünal, Sombor index over the tensor and Cartesian products of monogenic semigroup graphs, *Symmetry*, **14** (2022), 1071. https://doi.org/10.3390/sym14051071

32. A. Q. S. Alameri, M. S. Y. Al-Sharafi, Topological indices of some new graph operations and their possible applications, *Asian J. Probab. Stat.*, **13** (2021), 16–30. https://doi.org/10.9734/ajpas/2021/v13i230302

33. A. Alameri, M. Alsharafi, E. Ali, M. S. Gumaan, A note on topological indices and coindices of disjunction and symmetric difference of graphs, *Discrete Appl. Math.*, **304** (2021), 230–235. https://doi.org/10.1016/j.dam.2021.07.037

34. S. Hosamani, D. Perigidad, S. Jamagoud, Y. Maled, S. Gavade, QSPR analysis of certain degree based topological indices, *J. Stat. Appl. Probab.*, **6** (2017), 361–371. https://doi.org/10.18576/jsap/060211

35. S. Mondal, A. Dey, N. De, A. Pal, QSPR analysis of some novel neighbourhood degree-based topological descriptors, *Complex Intell. Syst.*, **7** (2021), 977–996. https://doi.org/10.1007/s40747-020-00262-0

36. A. Alameri, M. Alsharafi, *Topological indices types in graphs and their applications*, Mathematics Research Developments, Generis Publishing, 2021.

37. M. S. Y. Alsharafi, A. Q. Alameri, The F-index and coindex of V-Phenylenic Nanotubes and Nanotorus and their molecular complement graphs, *Nanosyst.: Phys. Chem. Math.*, **12** (2021), 263–270.

38. M. Alsharafi, Y. Zeren, A. Alameri, The second hyper-Zagreb index of complement graphs and its applications of some nano structures, *Asian J. Probab. Stat.*, **15** (2021), 54–75. https://doi.org/10.9734/ajpas/2021/v15i430364

39. M. Alsharafi, A. Alameri, Y. Zeren, M. Shubatah, A. Alwardi, The Y-index of some complement graph structures and their applications to nanotubes and nanotorus, *J. Math.*, **2024** (2024), 4269325. https://doi.org/10.1155/2024/4269325

40. A. Hakeem, A. Ullah, S. Zaman, E. E. Mahmoud, H. Ahmad, P. Ali, et al., Topological modeling and QSPR based prediction of physicochemical properties of bioactive polyphenols, *Sci. Rep.*, **15** (2025), 27466. https://doi.org/10.1038/s41598-025-11863-5

41. E. Alzahrani, M. F. Hanif, A machine learning framework for QSPR modeling of drug-like compounds using graph invariants, *AIMS Math.*, **10** (2025), 24651–24690. https://doi.org/10.3934/math.20251093

42. B. Song, J. Zhu, N. A. Azam, K. Haraguchi, L. Zhao, T. Akutsu, Cycle-configuration descriptors: a novel graph-theoretic approach to enhancing molecular inference, *J. Cheminform.*, **17** (2025), 125. https://doi.org/10.1186/s13321-025-01042-z

43. A. Altairi, Z. Alhaj, M. Alsharafi, Y. Zeren, From graph theory to chemoinformatics: modified bond-based indices and a hypothesis-driven multi-task QSAR/QSPR benchmark, *Sci. Rep.*, **16** (2026), 10104. https://doi.org/10.1038/s41598-026-40969-7

44. I. Tomescu, Graphs with given cyclomatic number extremal relatively to vertex degree function index for convex functions, *MATCH Commun. Math. Comput. Chem.*, **87** (2022), 109–114. https://doi.org/10.46793/match.87-1.109T

45. D. He, Z. Ji, C. Yang, K. C. Das, Extremal graphs to vertex degree function index for convex functions, *Axioms*, **12** (2023), 31. https://doi.org/10.3390/axioms12010031

Supplementary

The Cheméo-based dataset used in this study contains 89 unique compounds after duplicate removal. Physicochemical property values were compiled from Cheméo (`https://www.chemeo.com/`) using the units reported by the source. All data and materials required to reproduce the descriptor calculations and the exploratory QSPR analyses are provided as attached Supplementary materials.

Supplementary 1

`Supplementary1.xlsx`. A curated dataset containing the investigated compounds together with their molecular identifiers, molecular formulas, structural representations, elliptic Dharwad index values, and the compiled physicochemical endpoints used in the QSPR analysis.

Supplementary 2

`Supplementary2.ipynb`. A Jupyter notebook containing the Python workflow used for elliptic Dharwad index computation, dataset processing, model screening, repeated cross-validation, external test evaluation, and validation diagnostics for the *ED*-based QSPR study.